An Insight into the Battery Degradation and a Proposal for a Battery Friendly Charging Technique

Bikash Sah
IIT Guwahati
Praveen Kumar (praveen_kumar@iitg.ac.in)
IIT Guwahati

Research Article

Keywords: Battery, Battery Degradation, Charging Techniques, Electrochemistry, Fast Charging

Posted Date: July 13th, 2021

DOI: https://doi.org/10.21203/rs.3.rs-710085/v1

An Insight into the Battery Degradation and a Proposal for a Battery Friendly Charging Technique

Bikash Sah, Praveen Kumar
Department of Electronics and Electrical Engineering,
Indian Institute of Technology Guwahati, Assam, 781039, India

Abstract

Li-ion batteries are widely used in electric vehicles because of their promising characteristics that meet high specific power and energy density requirements. The only setback is the capacity fading due to degradation in Li-ion batteries. The rate of capacity fade in Li-ion batteries in EVs vary based on the charging rate, changes in internal cell temperature and external ambient temperature, and user driving patterns. Since the Li-ion battery is electrochemical, determining the actual cause of degradation at a particular instant and constraining the rate is a big challenge. Further, the causes are related to parameters which are chemical, electrical and mechanical. In this work, the causes of degradation are studied by analysing the variation of parameters for multiple charge types and rates at different ambient temperatures. The analysis leads to developing a new battery friendly charging scheme suitable to fast charge battery at different ambient temperatures appropriately and constrain battery degradation.

Lithium-ion batteries have shown promising characteristics to meet the requirements of both hybrid and battery electric vehicles[1,2]. Lithium-ion batteries were first commercialised in 1991 by Sony corporation[3]. Higher energy density, specific energy and power density of Li-ion batteries are the major reason for wide usage in EVs. The equivalent weight of the lithium metal compound (160 g Li/kWh) used in the battery's negative electrode is low compared to other chemistries of secondary batteries[4]. The size of the positive ion of lithium (0.74A°) is also very small, providing ease to diffusion and efficient intercalation and deintercalation of Li+ ions in electrodes of battery. The lower weight of Li metal leads to a higher energy density and specific energy, while the size of its ion helps increase the power density of the batteries. To date, researchers have proposed a variety of Lithium-ion chemistries that have either been commercialised or still under research[3,5]. The goals of the ongoing research in batteries for application in EVs are to improve the safety, thermal stability, energy density, rate of charge acceptance, cycle durability and reduce the manufacturing and environmental cost[2,6].

Although Li-based chemistry is commercially used in EVs, it has limitations that hinder the acceptance. The Li compounds and the materials required for manufacturing Li-ion batteries should have the least impurity. Further, metals like lithium, nickel, cobalt and manganese are also costly. Hence, the development and manufacturing processes of Li-ion batteries is high[7].

Capacity fade due to ageing and the change in its rate due to variation in ambient temperature are the major issues related to Li-ion batteries. Calendar and cyclic ageing are the two types of ageing characterised in batteries. Calendar ageing is linked to the storage conditions of batteries, state of charge (SoC), and the storage area's ambient temperature. A higher storage temperature and SoC instigates the secondary reactions[8]. On the other end, cyclic ageing is characterised by the degradation in the battery due to the charge-discharge cycle. Structural change in electrodes, solid electrolyte layer formation, chemical decomposition, or dissolution is a few resultants of cyclic ageing[9]. Capacity fade of Li-ion batteries is a widely researched topic in literature[10]. The literature highlights that the magnitude and pattern of applied current density, ambient and internal temperature of battery, packaging and mechanical stress have a major role in deciding the rate of capacity fade[11,12]. The discharge pattern of the batteries also impacts the capacity fade, but the pattern in an EV is based on the requirement of current to drive the motor in the powertrain. Hence, instead of studying capacity fade due to discharge pattern in an EV, the sizing of entities in a powertrain is widely studied.

The directions of research in capacity fade is diverse. Research in electrodes (material, structure, chemistry and binders), electrolytes (chemistry and additives), the structure of the battery, tabs, parameter estimation, electrochemical modelling, mechanical modelling, causes of capacity fade, electrical modelling and charging techniques are commonly found in the literature[11,13]. However, they have a common question to answer- how can the battery be charged at the fastest possible rate with minimum capacity fade? Fast charge and low capacity fade are opposing goals which is shown in Figure S.1. Figure S.1 shows the increase in the rate of capacity fade with an increase in the charging rate. An increase in the charging rate corresponds to a decrease in the time to charge.

Further, the battery is an electrochemical system. Hence it requires more profound insights into the chemical and mechanical changes occurring inside the battery to claim the causes of capacity fade. Chemical degradation and mechanical degradation are the two types of degradation reported in the literature.

The processes of chemical and mechanical degradation and their dependency on the charging techniques and the ambient temperature have been described in the literature. However, there is a lack of studies that provide a deeper insight by describing the variation of parameters of battery with change in charging technique. The parameters widely studied in the literature are inactive material, SEI layer thickness, overpotential, lithiation, porosity, tortuosity, and particle crack length[11,14–17]. The variation of the parameters results in the change in charging time, capacity, energy and power[16,18]. Moreover, the parameters are dependant on the ambient temperature of the battery. The studies related to the impact on the battery parameters with change in the ambient temperature are also missing in the literature. Hence, via this work, the authors describe the impact of C_rate on the rate of chemical and mechanical degradation, the suitability of charging techniques at different ambient temperatures, and the suitability of the type of charging for high power and low power application. Further, a new charging technique suitable for all applications and ambient temperatures is proposed to fast charge with constrained degradation.

Results

The parameters of Li-ion batteries studied in the literature are either electrical or electrochemical, or mechanical in nature. The electrical parameters studied are impedance, SoC, SoH, capacity (fade, retention, relative, incremental, utilisation), energy efficiency, variations in OCV voltage, and specific energy are. Electrochemical parameters include side reactions rate, overpotential, active material volume concentration in electrodes, SEI (thickness, density, film resistance, potential), lithium loss, side reaction exchange current density, electrode potentials, and polarisation voltage. Porosity, electrode particle cracking, structural disordering, stress and expansion of cell (width and length) are the mechanical parameters studied in the literature. The rise in temperature, change in charging time, and rate of capacity fade results from variation in these parameters.

The CC-CV is the oldest and standard technique described in the literature. Hence, all the new proposed charging algorithms in the literature compare the variation of parameters listed above with CC-CV. Moreover, impedance is the most commonly studied parameter in earlier studies because of the possibility to relate with the variation of SoC and battery degradation[17,19–22]. Table S.1 list the types of parameter studied for different types of charging techniques. Maximum parameters are studied in CC-CV charging technique being the oldest and a standard charging technique. In contrast, the least number of parameters are studied in the temperature-based charging technique[23].

The study of variation in the type of parameters for each charging technique is associated with the rate of battery degradation. Although the literature has described multiple studies on each charging technique to prove the suitability of fast charge and reduced battery degradation, there are lack of studies that associate all the three types of parameters - electrical, chemical, and mechanical. Further, only a few works describe the effect on the parameters due to an increase or decrease in the ambient temperature. Hence, the commercially used charging techniques- CC, CCCV, pulse charging (with negative pulse and without negative pulse) and variable frequency/duty charge pulse will be analysed in detail to understand and associate the change in the three types of parameter with degradation phenomenon.

In this work, overpotential, the extent of lithiation in electrodes, inactive material volume fraction, SEI layer thickness in electrodes are studied as chemical parameters. The porosity, tortuosity, and the phenomenon of particle cracking in the electrodes are included in mechanical parameters, while the resultant parameters such as energy, power and capacity fade are analysed as electrical properties. Li-ion batteries undergo two reactions during charging and discharging- primary intercalation reactions and secondary electrochemical reactions (also called as side reaction). The intercalation reactions are responsible for the charge and discharge of batteries. In contrast, the side reactions lead to the loss of lithium and active materials, which intervenes in intercalation reactions. It also leads to electrolyte oxidation and reduction, passivation, structural disordering, particle cracking and thickening of the SEI layer. The resultants of side reactions lead to the capacity fade in the battery, which will be described in the subsequent subsections. SEI layer thickness, particle cracking, change in internal cell temperature are the major parameters impacting the capacity fade of the batteries. Hence, they are included in the main study while others are described in the supplementary section.

SEI layer thickness

Side reactions in Li-ion batteries occur in three major regions viz. electrode-electrolyte interfaces, electrode-collector interface and electrolyte[24]. Change in the equilibrium potential of the reactions during charging and discharging leads to instability in the electrolyte. The instability is accompanied by the start of side reactions within battery[25]. The change in the equilibrium potential depends on the amplitude of the charging current and the types of charging. Hence, the concentration of the inactive materials and electrode-electrolyte interfaces or SEI layer thickness varies for different charging types and rates. Although the SEI layer is a by-product of side reactions, it is a required protective layer in graphite particles of negative electrodes in the battery. The lithium potential makes the electrolyte unstable and vulnerable to the reaction, which leads to the loss of lithium and a reduction in the overall capacity of batteries. Since it is a form of inactive material, the variation of the concentration of inactive material and the thickness of SEI layer are similar as shown in Fig. S.5 and Fig. 1a. The thickest SEI layer is formed in CC and CCCV, followed by CT9, which is pulse charging with discharge. The SEI layer thickness for all charging rates is also highest in CCCV. During CCCV, the time for the CV phase is higher and increases with an increase in the number of cycles. During CV, the stress due to electrochemical reactions and temperature is lower than the CC phase, leading to stable SEI formation[9,26]. Hence,

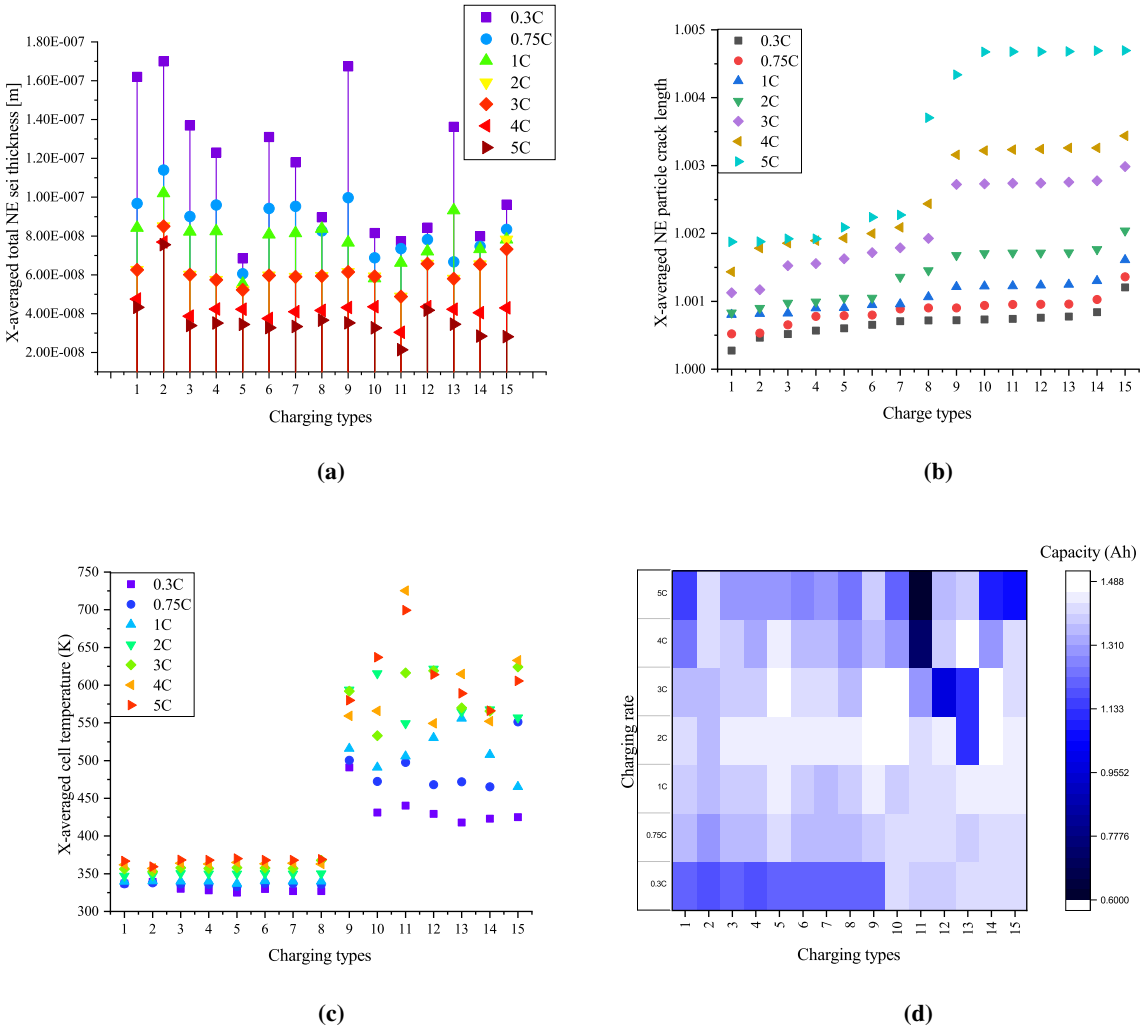

Figure 1: Variation of parameters of the batteries at different charging techniques and charging rates : (a) The X-averaged total negative electrode SEI thickness [m] decreases with increase in C_{rate} as the chemical degradation is dominant at slower C_{rate}; (b) X-averaged negative electrode particle crack length increases with increase in C_{rate} because of the increased stress in electrode particles; (c) X-averaged cell temperature [K] is higher for higher C_{rate} due to the increase in chemical kinetics. The discharge pulses further instigates the phenomenon because of the change in the direction of motion of ions and masses;(d) Capacity is a function of chemical and mechanical parameters and internal change in temperature.

Table 1: Summary of the variation of parameters with increase in the charging rate in different charging techniques. †, $^{\#}$, $\Downarrow$, $\Uparrow$, and * resembles decreasing, increasing, decreasing trend, increasing trend and negligible change, respectively.

Sl. No	Parameters	CC	CCCV	Pulse charging without discharge					Pulse charging with discharge			
									Amplitude of discharge current			
		$C_{rate}{}^{\#}$	$C_{rate}{}^{\#}$	$t_{on}{}^{\dagger}$	$t_{on}{}^{\dagger}$	t_{on} & $t_{off}{}^{\dagger}$	$C_{rate}{}^{\#}$	t_{on}	0.5	1	2	$C_{rate}{}^{\#}$
1	X-averaged negative electrode inactive material volume fraction	$\Downarrow$	$\Downarrow$	$\Downarrow$	$\Downarrow$	$\Downarrow$	$\Downarrow$	$\Downarrow$	$\Downarrow$	$\Uparrow$	$\Downarrow$	$\Downarrow$
2	X-averaged total negative electrode SEI thickness [m]	$\Downarrow$	$\Downarrow$	$\Downarrow$	$\Downarrow$	$\Downarrow$	$\Downarrow$	$\Downarrow$	$\Downarrow$	$\Uparrow$	$\Downarrow$	$\Downarrow$
3	X-averaged negative electrode porosity	$\Downarrow$	$\Downarrow$	$\Downarrow$	$\Downarrow$	$\Downarrow$	$\Downarrow$	$\Downarrow$	$\Downarrow$	$\Uparrow$	$\Downarrow$	$\Downarrow$
4	X-averaged negative electrode tortuosity	$\Uparrow$	$\Uparrow$	$\Uparrow$	$\Uparrow$	$\Uparrow$	$\Uparrow$	$\Uparrow$	$\Uparrow$	$\Downarrow$	$\Uparrow$	$\Uparrow$
5	X-averaged negative electrode reaction overpotential [V]	$\Uparrow$	$\Uparrow$	$\Downarrow$	$\Downarrow$	$\Downarrow$	$\Uparrow$	$\Downarrow$	$\Uparrow$	$\Downarrow$	$\Uparrow$	$\Uparrow$
6	X-averaged negative electrode extent of lithiation	$\Downarrow$	$\Downarrow$	$\Downarrow$	$\Downarrow^{*}$	$\Downarrow$	$\Downarrow$	$\Downarrow$	$\Downarrow$	$\Uparrow$	$\Uparrow$	$\Downarrow$
7	X-averaged cell temperature [K]	$\Uparrow$	$\Uparrow$	$\Uparrow$	*	$\Downarrow$	$\Uparrow$	Low C_{rate} =$\Uparrow$ and High C_{rate} =$\Downarrow$	$\Downarrow$	Low C_{rate} =$\Uparrow$ and High C_{rate} =$\Downarrow$	$\Downarrow$	$\Uparrow$
8	Capacity fade	$\Uparrow$	$\Uparrow$	$\Downarrow$	$\Downarrow^{*}$	$\Downarrow$	$\Uparrow$	$\Uparrow$	$\Downarrow$	$\Uparrow$	$\Uparrow$	$\Uparrow$
9	X-averaged negative electrode particle crack length	$\Uparrow$	$\Uparrow$	$\Uparrow$	$\Uparrow$	$\Uparrow$	$\Uparrow$	$\Uparrow$	$\Downarrow$	$\Uparrow$	$\Uparrow$	$\Uparrow$

with an increase in the number of cycles, the SEI layer keeps becoming thicker. Further, the formation of SEI is also higher at lower charging rates for the same reason as seen in Fig. 1a.

The plot in Fig. 1a shows that pulse charging has the potential to reduce the SEI layer thickness. The SEI layer thickness in charge type 3 to 8, which is pulse charge without discharge, varies with the change in the t_{on}. The thickness is highest in charge type 3, which has the maximum t_{on}, while charge type 5 has the lowest because of the least t_{on}. The t_{off}, too, impacts the thickness of the SEI layer. With a decrease in the t_{off}, the SEI layer thickness is reduced. A reduced t_{on} as well as the t_{off} help to suppress the thickness of the SEI layer. A larger t_{on} at a lower C_{rate} act similar to CCCV. Even at a higher C_{rate}, the rest phase of the pulse will help to stabilise the SEI layer leading to thickening with an increase in the number of cycles. Hence, a decrease in t_{on} and t_{off} help reduce the SEI layer's thickening.

The variation in the change of SEI layer thickness for pulse charging with discharge is shown in charge type 9 to 15 in Fig. 1a. Majority of the pulse charging with discharge charge type help in reducing the SEI layer thickness. The SEI layer thickness has a reducing trend for charge type 9 to 11, although the variation is not much for charge type 10 and 11. The amplitude of discharge current, too, had a role in the change in the SEI layer thickness. When the amplitude of the discharge current is equal to the average current (charge type 9 to 11), with the reduction in t_{on}, the SEI layer thickness is also reduced.

Further, when the amplitude of the discharge current is equal to half of the average current (charge type 12 and 13), a higher on-time resulted in less SEI layer thickness. On the contrary, when the amplitude of discharge current is equal to the twice average current, a higher on-time resulted in a thicker SEI layer. The change in the polarity of the charge pulses leads to a similar variation of equilibrium potential. When the amplitude of the current in the discharge pulse is more than the charge pulse, the equilibrium potential falls below the electrolyte's stability limits, accelerating the SEI formation. The rest phase further helps to stabilise the SEI formed, leading to a thick SEI layer in comparison when the amplitude of the current in the discharge pulse is less than or equal to the charge pulse. The charge type with amplitude of discharge current equal to the average current and least t_{on} and rest time have thinnest SEI layer formed over the negative electrode.

Particle crack length

Particle cracking is a form of mechanical degradation in battery observed in the electrode particles. The stress in electrode particle are commonly modelled or experimentally reported due to intercalation/deintercalation reaction and changes in internal cell temperature variations or ambient temperature variations[27]. The crack in the particles results in exposure to the surface of active materials leading to side reactions. These side reactions further lead to heat generations, amplifying the phenomenon of stress and side reactions due to an increase in cell kinetics[28]. Hence, an increase in mechanical degradation increases the chemical degradation and vice-versa, but each degradation depends on the C_{rate}.

Fig. 1b shows the variation of particle crack length on the application of different types of charging techniques at

different charging rates. The slower charging rates resulted in the least particle cracking. There is an increase in the particle crack length on going from left to right. The CC and CCCV resulted in the least crack length, although CCCV has higher values when compared to CC. Since at higher potential of battery, the stress on the particles of electrodes is higher, CCCV resulted in higher crack length. In CC, the battery is allowed to settle with a reducing charge current. Since the battery is not allowed to settle and overpotential remains higher, the stress due to increased potential of battery and saturation of electrodes is not experienced. While in the case of CCCV, the battery keeps on charging after switching to CV. With increase in potential, the stress on particles of electrodes continue to increase. Hence, the particle crack length is more than CC.

The pulse charging techniques that resulted in a better candidate for fast charge when previous parameters were considered do not perform well. The reason behind the increase in the crack is related to the heat generation during the intercalation and deintercalation reaction. The heat generation adds to the internal battery temperature rise, increased chemical kinetics, and stress in the electrodes particle. The higher the rise in internal cell temperature (Fig. 1c), the higher is the particle crack length. Hence, a change in the ambient temperature might result in an increase or decrease in particle cracking. During pulse charging with discharge, the increase in the amplitude of the discharge pulse resulted in a further increase in the particle crack length.

Cell temperature

The internal cell temperature is a major factor impacting the capacity fade of batteries. The temperature brings changes in equilibrium potential of reactions within the battery, the chemical kinetics which affects the rate of side reactions, SEI layer formation and erosion, the diffusivity of charge and mass in electrodes, stress in battery, structure disordering in electrodes and overall geometry, and safety in the operation of battery[1,29,30].

A higher C_{rate} resulted in an increase in the heat generation due to rapid diffusivity of charges and increased stress in the electrode particles. The conventional CC and CCCV had control on the rise in the internal cell temperature. However, during pulse charging with discharge, the temperature rose to a very high value. The temperature rise is related to the ease in the diffusivity of charge in the battery both during intercalation and intercalation. With an increase in the SEI layer thickness, decrease in porosity and increase in the tortuosity of electrodes, the charge and mass transfer are offered resistance. The increase in the resistance adds to the heat generation and impacts the stability of electrolyte.

The impact of the increase in internal cell temperature is deteriorating in nature. The increase in the temperature induces stress in the electrode particles and erodes the SEI layer. On erosion, the surface of active material or electrode particles are unlatched to further side reactions. Apart from forming the SEI layer, the side reactions leave behind residual inactive materials and gases, which are generated due to phase transition from solid to gas or liquid to gas. An uncontrolled rise in the temperature is imperative to lead to thermal runaway and harm the safety of the battery being charged pr discharged. Fig. 1c infers that conventional CC and CCCV and pulse charging without discharge are effective methods to perform fast charge with a limited rise in internal battery temperature.

Discharge capacity

Discharge capacity is the final parameter of the battery, which determines the performance of the battery. Discharge capacity depends on various parameters discussed in previous subsections. The reduction in capacity fade depends on the C_{rate} and the types of charging techniques as shown in Fig. 1d. The C_{rate} impacts the rate of chemical kinetics, equilibrium potential and stress due to intercalation reactions. An increase in the mentioned parameters increases the overpotential while vice-versa reduce the overpotential. At higher C_{rates}, the overpotential rises and leads to an increase in the terminal voltage. Since the battery terminal voltage reaches the cut-off potential much earlier, the electrode is not lithiated fully. The battery does not charge to the full range of SoC. When CCCV is used to charge, the CV part of charging allows the battery to be charged in a wider SoC range as the rise in overpotential is countered by a fall in current. Further, the time to charge also impacts the reduction in discharge capacity. A larger time period will lead to increased stress on electrode particles due to increased concentration gradients[31]. Increased stress adds to SEI erosion and further side reactions leading to loss of active particles and Li-ions[26].

In Fig. 1d, it can be seen that CCCV leads to larger capacity loss at slower C_{rate} when compared to CC, but at a higher C_{rate}, the CC leads to larger capacity loss. A similar pattern is seen in the case of pulse charging without discharge also. The t_{on} and t_{off} time also impacts the reduction in discharge capacity. A decrease in t_{on} and t_{off} are instrumental in countering the reduction in discharge capacity. Contemplating, it is observed that higher charging rates are a possible solution with pulse charging without discharge. However, 2C is found to be an optimal C_{rate}.

Looking into the pulse charging with discharge, an increased t_{on} leads to a similar pattern of reduction in discharge capacity. The reduction in t_{on} helps to reduce the rate of reduction of discharge capacity. The amplitude of discharge pulse during charging too impacted the change in discharge capacity. When the amplitude of discharge pulse is more than or equal to the average charging current, the discharge capacity reduces drastically. The drastic reduction can be related to the change in the equilibrium potential of reactions and the overpotential during charge, rest and discharge durations. The rise in internal cell temperature due to an increase in cell kinetics cannot be neglected while selecting an optimal charging technique to fast charge. The pulse charging with discharge increases the internal cell temperature to

a higher value, leading to thermal runaway. Considering the reduction in discharge capacity, CT5 is the best technique to charge the battery at higher C_{rate}.

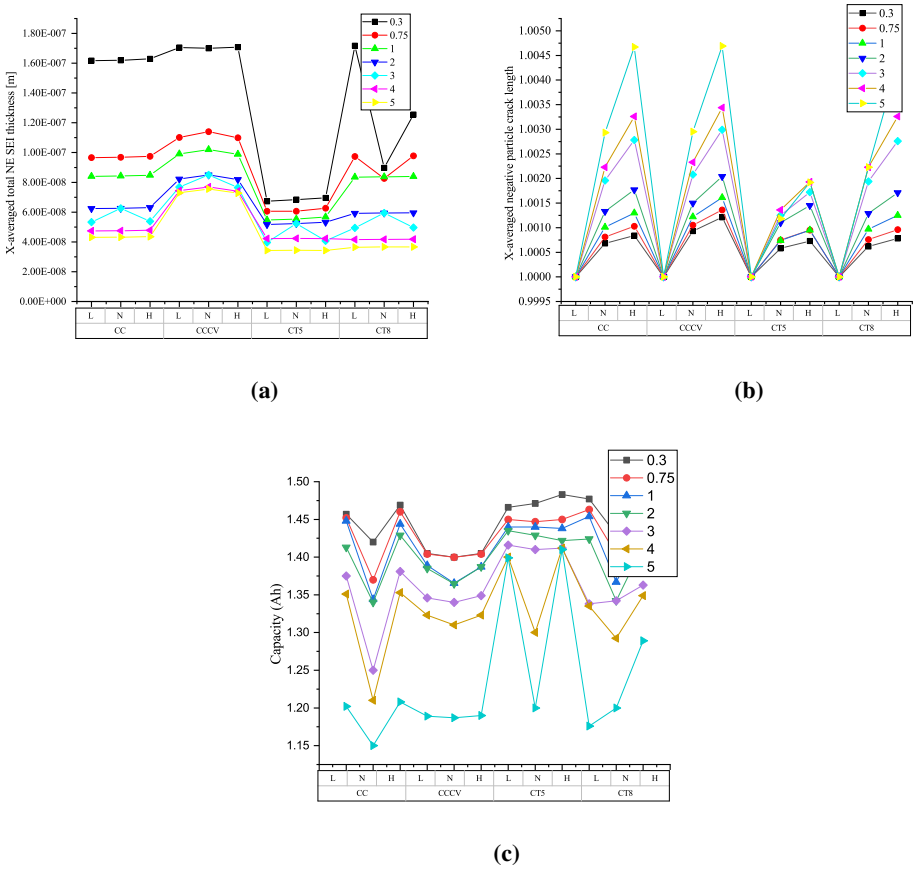

Figure 2: Variation of different parameters of the batteries: (a) An appropriate value of t_{on} and t_{off} help in reduction in the X-averaged negative electrode SEI thickness [m]; (b) The X-averaged negative electrode particle crack length is also least when CT5 is used; (c) The variation of capacity fade is the most at higher C_{rate}, and CT5 is found to be helpful in constraining the rate of capacity fade.

Comparison of the results with the change in ambient temperature

Various works in literature have reported the impact of ambient temperature in operation and ageing mechanisms of the battery at different C_{rate}. However, the effect of the charging types is not a widely discussed topic in the literature, although a few works suggest charging techniques for extreme temperature conditions[32,33]. Hence, this work is further extended to analyse the impact of the charging technique at two extreme temperatures - 318.15 K (45 ^{o}C) and 273.5 K (0 ^{o}C). The temperature changes the rate of formation of inactive materials, including SEI, erosion or decomposition of SEI and instability in electrolyte resulting in reduction reactions with active material. Rise of internal temperature above a certain level (125^{o}C to 180^{o}C) can lead to thermal runaway, venting, and complete damage of battery[34].

The previous results, which were at 298.15 K (25 ^{o}C), are compared with the results obtained at two extreme temperature for selected four types of charging techniques. CT5 and CT8 variants of pulse charge with discharge resulted in the best performing charging types based on the previous simulations at normal ambient temperature. Hence, to reduce the simulation time, further simulations are performed on only four types of charging techniques, viz. CC and CCCV being conventional, and CT5 and CT8 are only simulated at two extreme temperatures. CT5 and CT8 are found to be the best charging types based on the analysis performed in previous subsections.

Fig. 2 and Fig. S.10 shows all the parameters studied to determine the performance of the battery at different charging rates and temperatures. Three different temperatures are represented by ”L” (273.5 K (0 ^{o}C)), ”N” (298.15 K (25 ^{o}C)) and ”H” (318.15 K (45 ^{o}C)). The parameters analysed are those presented in Fig. 1. The difference in the formation of inactive material for different C_{rate} is the least in the case of CT5. For CC, at lower C_{rate}, the variation in the formation of inactive material is negligible with a change in the temperature. The change in overpotential of the battery is also less; thereby, the changes in SEI layer thickness, porosity, and tortuosity also follows a similar pattern. The parameter which shows differences are the lithiation, particle crack length and capacity. The changes in the lithiation is related to the rate of diffusivity, which changes with the change in the temperature. At lower temperature, higher resistance to diffusivity is found in the batteries, resulting in decreased lithiation. With an increase

in the temperature, the Li-ions and mass transfer rate increases with an increase in chemical kinetics. As the lithiation increases, there is an increase in the stress in the particles of the electrode. Hence, as expected, the particle cracking increases with the temperature.

The changes in temperature does not results in a major change in the parameter when CCCV is used, although there is a rise in the formation of inactive materials, SEI layer thickness, overpotential, lithiation and tortuosity. Porosity decreases while particle crack length does not show any major difference with CC. CT5, which is found to be the best charging technique, shows the least variation in values of parameters at different charging rates. The decrease in the t_{on} and t_{off} resulting in the changes as described in previous subsections. The results with reduced t_{on} and t_{off} aligns with the finding in[35] where it is shown that a low-frequency diffusion leads to higher impedance of the battery. The impedance of the battery is due to an increase in the growth of the SEI layer and the formation of inactive materials. CT8, which follows the CT5 in performance, has a similar results pattern as found in CC, CCCV and CT5.

Suitability of type of charging for high power or high energy applications

The degradation of Li-ion batteries in EVs also depends on the application. The EVs in transport sector ranges from small two-wheeler to large bus application. The fast EV racing cars are not far behind in tracks. The variation in the requirements of torque and speed of EV motor changes the discharge pattern of batteries. Hence, the rate of degradation also varies for the same battery used in a different application. In this work, an analysis to determine the performance of battery for the higher energy or higher power applications is also done. Fig. 3 shows the plot of terminal power vs energy plots for different charging techniques and C_{rate}.

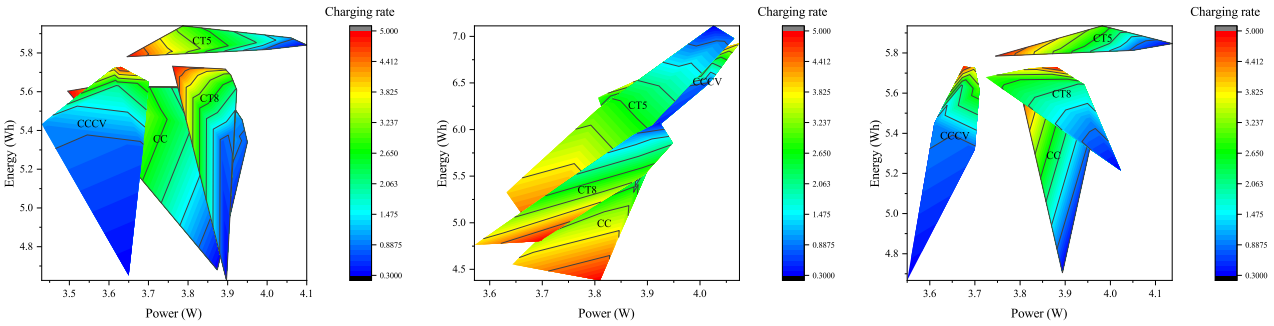

Figure 3: Variation of terminal power and energy of the battery for different charging techniques and charging rate at different temperatures (a) Energy vs power plot at very low ambient temperature; (b)Energy vs power plot at normal ambient temperature; (c)Energy vs power plot at high ambient temperature

Fig. 3a shows the plot for lower ambient temperature. CT5 performs the best up to $2C_{rate}$ for all the temperature conditions under study. The CCCV becomes a competitor at normal temperature conditions, but CT5 still outpaces. Further, CCCV is performs worst at low and high ambient temperature regions. The results clearly depict the requirements of different charging pattern for different types of vehicles. Fig. 3b is the plot for normal ambient temperature range. CT5 and CCCV are close competitors while CT8 and CC are far behind and not suitable for use. From Fig. 3c, which is the plot for higher ambient temperature range, CT5 resulted in the best charging technique. The higher charging rate still remains a challenge for all the ambient temperature conditions. The solution to the problem is discussed in the next section.

Discussion and outlook

The benefits of Li-ion batteries and their wide application in EVs have developed research interest to meet the challenges. All the challenges in EVs converge to one- rate of battery degradation[1,2,9,36]. The rate of battery degradation changes with the change in utilisation of EV battery. The utilisation depends on the EV driver behaviour, temperature of the environments and type of utilisation of EVs (high energy or high power applications). Higher energy and power density requirements result in a series-parallel connection of cells, which adds to the challenges of making the pack safe, durable, and lower cost[1]. The battery degradation is triggered by the change in the equilibrium potential of the reactions in the battery. The thermodynamic force to drive the reactions in the battery is associated with equilibrium potential. Hence, changes in the internal battery or external ambient temperature lead to a variety of chemical and structural alternations[37].

An increase in the temperature leads to heighten kinetics of both intercalation-deintercalation and side reactions. The inactive material formed during elevated temperature has a different morphology in comparison with normal temperature. Most importantly, the SEI layer composition changes. Studies are performed using differential scanning

calorimetry and accelerated rate calorimetry to determine the cell or electrode behaviour[38–40]. These studies disclosed the phenomenon of self-heating due to exothermic side reactions. The selection of electrolyte salt has a significant role in the temperature rise. The elevated temperature further erodes the existing SEI layer over the active material. The eroded SEI either dissolve or re-precipitate, leading to the restructuring of damaged SEI and more side reactions. More stable SEI and inorganic products are formed, such as lithium fluoride and lithium carbonate[41]. Further, these stable products are less penetrable for Li-ions, thereby decreasing SEI's overall diffusivity and ionic conductivity.

At low temperatures, the degradation of the battery is not dominated due to changes in the SEI formation instead by the phenomenon of lithium plating and dendrite formation[16,42]. This study does not consider these two phenomena. Hence the related results are not presented. However, the literature states that, at low temperature, the equilibrium potential of intercalation reactions drops close to the lithium metal potential[43]. Further, the viscosity changes in the electrolytes are observed, leading to a decrease in the diffusivity of li-ion into electrolytes and electrodes[44]. Li-metal reactions in the electrolyte lead to side reactions, which accelerated the ageing process and increased capacity loss. The saturation of electrodes due to slow diffusion and Li's settlement around electrodes adds to the increase in local potential. Hence, the possibility of Li metal plating or dendrite formation increases.

The discussions in this subsection help gain insights into different types of charging techniques discussed in this work. The conventional techniques viz CC and CCCV have shown increased chemical degradation during lower C_{rate} and increased mechanical degradation during higher C_{rate}. The inactive materials and SEI layer formed at all the C_{rate} is higher when compared to pulse charging without discharge, as seen in Fig. S.10a and Fig. 2a. Similarly, the particle cracking length is also higher. The CT5 has shown the best results in terms of all the parameters analysed in Fig. 2. Even when the ambient temperature is taken into consideration, the performance does not deteriorate. Hence, pulse charging technique without discharge pulse with a reduced t_{on} and t_{on} can be a suitable option to go for fast charging and constrain the battery degradation. The value of t_{on} and t_{off} is an optimization problem given in[45].

Although the CT5 results are optimal for all temperature conditions analysed in this work, the design of new charging techniques will be indispensable at extreme temperatures such as -20 ^oC and 80 ^oC. Further, each charging technique has advantages and disadvantages that can be utilised to charge in extreme environmental conditions. The amalgamation of the charging techniques directs us towards the developing a new rule-based charging strategy for Li-ion batteries. Further, for high energy and high power applications as well, the rules can be framed by selecting the suitability of charging type from Fig. 3, monitoring the rise in internal battery temperature, and appropriately varying the C_{rate}.

The rule-based charging strategy should incorporate the battery electrochemistry, present battery health parameters, environmental conditions, user requirements and grid conditions. Hence, a new rule-based charging strategy is proposed to fast charge with reduced battery degradation in this work. Different types of electrochemistry of Li-ion battery are commercially available such as Lithium Cobalt Oxide (LCO), Lithium Manganese Oxide (LMO), Lithium Iron Phosphate (LFP), and Lithium Titanate (LTO). The battery electrochemistry is to be considered because of the variation in ability to fast charge, performance, lifespan, specific power, and energy. The present battery health conditions will help to determine the ageing of the battery. Capacity estimated by the BMS or any types of the model or the previous battery charge and discharge profile data will help determine the battery's ageing. The environmental condition includes the temperature of the region. User requirements can be a fast, medium and slow charge. The grid conditions should also be incorporated to avoid the impact of uncoordinated charging, which leads to voltage imbalance and instability[46–48]. The electric grid can be at peak load, off-peak load or normal condition.

Assume an EV arrives at a charging station with lithium-titanate-oxide (LTO) battery electrochemistry. The battery is new and can charge to full capacity as communicated by the BMS. The temperature of the region of the charging station is below normal (-10 ^oC). The user opts to fast charge, and the grid is at peak load condition. For the given scenario, if a fast charge is performed, the grid will be overburdened. Hence, the user will be given an option to go with a slow or medium charge rate. If the user wants to continue the fast charge, the service will not be denied, and fast charging will be selected. The only condition to be evaluated is the ambient temperature. Since the temperature is very low, the battery is under stress, and the internal resistance is high. The rise of the internal resistance is due to the low ionic and mass diffusivity. Suppose the battery's internal temperature is increased, the viscosity of the electrolyte and the overall rate of diffusion can be brought to normal. The analysis in the previous subsection has shown that pulse charging with discharge can help in increasing battery's internal temperature. Hence, the battery undergoes a pulse charging with discharge for a period of time until the battery's internal temperature becomes normal. Later, with controlled battery temperature monitoring, fast charging can be performed using a charging pattern, leading to the least battery degradation. For instance, in this work, CT5 is found to be the best performer. Similarly, for LTO battery, an optimal charging pattern can be proposed.

The advantages of the rule-based charging system lie in the ease of implementation. The charging station developer can predefine a set of rules based on the changes in the climatic condition, nature of the user and their requirements of fast charge, condition of the electric grid over a period of time. The charger should be designed to meet the requirements of different charging strategies. A set of rules can be framed and fed to the controller of the charger. Every time a user connects for the charge, as per requirements, the rule will ensure the best services for both EV user and the electric grid. The assurance of the least battery degradation will advantage the EV user, and the electric grid will have the least impact of uncoordinated fast charge.

The disadvantages of such rule-based charging are data requirements related to battery parameters that need to be considered to fast charge with constrained battery degradation. Further, robust communication needs to be established

with the grid for real-time monitoring of connected load. The charger should also be capable of communicating with EV battery BMS. A computational signal processing board or connected infrastructure is also required to monitor and control the charging of EV batteries. These requirements make the charging systems costly, but an increase in cost will be compensated by avoiding ageing of battery and losses of power system operators due to uncoordinated charging.

Table 2 shows a rule base developed considering all the five parameters.

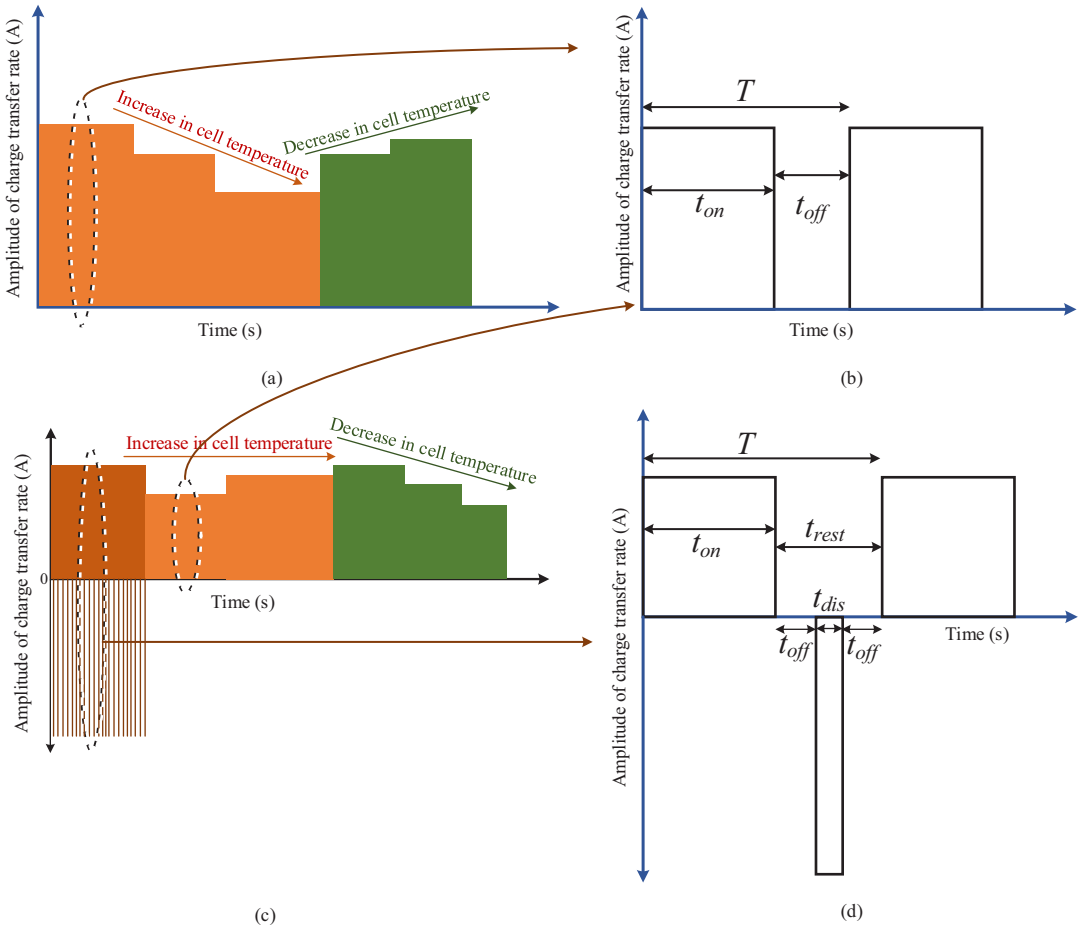

Figure 4: Proposed charging technique: (a) The charging pattern that is suitable for charging at normal or high ambient temperature. The increase and decrease in cell temperature is countered by reducing and increasing the amplitude of positive pulse current. (b) The pattern of pulse in which T, t_{on} and t_{off} are required to be computed to constrain battery degradation. (c) The charging pattern that is suitable for charging at extreme low temperatures. The discharge pulse of more than average charging current help to increase internal cell temperature. The increase and decrease in this case is controlled by shifting from pulse charging with discharge to without discharge and increasing or decreasing the amplitude of charge current.

Methods

A brief literature, the modelling of battery and the types of charging is discussed in this section. Fig. S.2 shows the structure of a Li-ion battery, which comprised of two electrodes, an electrolyte and a porous separator. The electrodes are made using active material particles held together using binders, and their structure help in storing lithium. Current collectors are connected to the electrodes for electrical connection. The direction of flow of lithium determines the state of charge and discharge in the battery. During discharge, the intercalated lithium in the negative electrode diffuses to the surface, initiating an electrochemical reaction. The electrochemical reaction leads to the release of Li^+ ion and an electron. The electrolyte prevents the flow of electrons but allows Li^+ ion to diffuse towards the positive electrode. Hence, the electron via the electrode and current collector travels to the positive electrode. At the surface of the positive electrode, the Li^+ ion combines with the electron to form a lithium atom and intercalate in the positive electrode particle. The process reverses in the case of charging.

Apart from the required electrochemical reactions to charge and discharge, Li-ion batteries undergo various undesirable reactions called the secondary reactions, which are not desirable. These secondary reactions are a major reason for battery degradation. The amplitude, frequency, and time to charge or discharge impacts the rate of secondary reactions, leading to two types of degradation mechanism, viz. chemical and mechanical. Further, the temperature and states of the battery also impact the rate of either degradation mechanism. Chemical degradation dominates at a lower applied current at normal ambient temperature, while a higher applied current and higher ambient temperature lead to fast mechanical degradation[31,49]. Hence, changing the pattern of current while charging is often explored to reduce the degradation of batteries.

Fig. S.4a shows the different types of charging proposed in the literature to fast charge and control the degradation of the battery. The charging techniques can be classified into conventional, active control, sinusoidal ripple, boost, constant temperature-constant voltage (CT-CV) and model-based charging. Each type of charging technique is proposed to increase the charging efficiency, reduce charging time, and reduce battery degradation in comparison to conventional techniques (mostly CC-CV).

Constant current (CC) was the first technique to charge the battery. The battery is considered to be fully charged when charging with a constant current leads to an increase in terminal voltage to a fixed cut-off voltage. Since, the battery is an electrochemical system, it experiences a reduction

Table 2: Example rule set for charging: The set of rules are designed based on the results obtained for the selected battery in this work. The user selection is not demonstrated in the process when the grid is in peak load hours. Further, frequency, duty cycle of the pulses and amplitude of charge and discharge pulse should be either computed online by preset optimisation algorithms or set as a predefined value determined based on experiments/simulations for any charge technique (CT5, CT9 or any pulse charging with discharge) defined in the table.

Sl.No	Present battery health	Environmental condition	User requirement	Charge technique
1	New	Low	Fast	Start charging by a high charge current pulse or pulse charging with discharge (similar to CT9*). With an increase in the internal cell temperature, charge technique similar to CT5* can be used to fully charge.
2	New	Normal	Fast	Start charging with charging technique similar to CT5*.
3	New	High	Fast	Start charging by a technique similar to CT5* and monitor the internal temperature. With the rise in the internal cell temperature, the C_{rate} should be reduced to constrain the rise. On stabilising the rise in internal cell temperature, C_{rate} can be increased again.
4	Half-life	Low	Fast	Start charging by using a technique similar to CT9*, with amplitude of discharge pulse lower than the average charge current. Monitor the rise in internal cell temperature. With the rise in internal cell temperature, shift charging to CT5. The internal cell temperature should be monitored to reduce C_{rate} on a rapid rise.
5	Half-life	Normal	Fast	Start charging using a technique similar to CT5 while monitoring the internal cell temperature. An increase in internal cell temperature near stability limits should be constrained by reducing C_{rate}.
6	Half-life	High	Fast	Start charging using a technique similar to CT5 and monitor the rise in internal temperature. Constrain the rise in internal cell temperature by reducing the C_{rate}. On decreased and stabilising the internal cell temperature, C_{rate} can be increased.
7	Degraded	Low	Fast	Start charging by deploying pulse charging with the discharge with amplitude of discharge pulse higher than the average charge current. The rise in internal cell temperature should be monitored. The charging should shift to a technique similar to CT5 on rise in temperature. The internal cell temperature should be monitored and a reduction in C_{rate} should be used to constrain the rise.
8	Degraded	Normal	Fast	The charging should be performed using a technique similar to CT5 and internal cell temperature should be monitored. C_{rate} should be decreased to constrain the rise in internal cell temperature after a certain safe value.
9	Degraded	High	Fast	The charging should start by a technique similar to CT5 and internal cell temperature should be monitored. With an increase in the internal cell temperature above a certain safe value, the C_{rate} should be reduced. The C_{rate} can be increased again once the cell reaches the level of normal internal cell temperature.
10	New	Low	Slow	Start charging using a technique similar to pulse charging with the discharge with amplitude of pulse discharge greater than the average charge current. The rise in temperature should be monitored and with an increase, shift to a technique similar to CT5. The C_{rate} should be decreased if the rise in internal cell temperature is observed around stability limits.
11	New	Normal	Slow	A technique similar to CT5 should be used to charge and regular monitoring of rise in internal cell temperature should be done. The rise in internal cell temperature near stability limits should be constrained by decreasing C_{rate}.
12	New	High	Slow	Start charging using a technique similar to CT5 and monitor the rise in internal cell temperature. Reduce C_{rate} to control the rise in internal cell temperature.
13	Half-life	Low	Slow	The charging should start using a pulse charging with the discharge with amplitude of pulse discharge greater than the average charge current. The rise in internal cell temperature should lead to shifting to CT5 or CT8. Reduce C_{rate} to control the rise in internal cell temperature.
14	Half-life	Normal	Slow	The charging should be done using a technique similar to CT5. The internal cell temperature should be monitored and C_{rate} should be changed to constrain the rise in internal cell temperature.
15	Half-life	High	Slow	Start charging using a technique similar to CT5 and monitor internal cell temperature. Modify the C_{rate} to control the rise in internal cell temperature.
16	Degraded	Low	Slow	Start charging using pulse charging with the discharge with amplitude of discharge pulse higher than the average charge current. Monitor the rise in internal cell temperature, and shift charging to CT5 once temperature rises. The internal cell temperature should be monitored to modify the C_{rate} on rise around safety limits.
17	Degraded	Normal	Slow	A A charging technique similar to CT5 should be performed with monitoring of internal cell temperature. The C_{rate} should be modified to constrain the rise in internal cell temperature above safety limits.
18	Degraded	High	Slow	Start charging similar to CT5 and monitor the rise in internal cell temperature. With an increase in the internal cell temperature around safety limits, the C_{rate} should be reduced and on reaching normal internal cell temperature, C_{rate} can be ageing increased.

in open-circuit voltage after a specified time of turn off. Hence, and a new technique of constant current-constant voltage (CC-CV) was proposed in which the battery is charged with a fixed value of current up to the specified cut-off voltage during CC[22,50]. On reaching cut-off voltage, the CV gets activated in which the voltage is kept constant and current starts reducing. At a specified value of current (50 mA), the battery is considered to be fully charged[20]. The reduction of current in the case of CV significantly increases the charging time. However, it allows the settling of mass and ions in battery, helping to reduce the concentration gradients within the electrode, and leading to more energy storage for a specified maximum voltage. The simplicity in implementing CC-CV and its ability to transfer more energy to the battery has made it a standard charging protocol for charging[51].

The idea of settling of ions or mass in battery is further exploited in pulse charging by the researchers. In pulse charge, the continuous current is interrupted periodically to give rest phases or discharge pulses[52,53]. These rest phases and discharge pulses help to settle the kinetics of ions and compounds in battery. Three types of pulse charging are reported in the literature: pulse charging without discharge, pulse charging with different current amplitude stage, and pulse charging with short discharge pulses[54,55]. Fig. S.4 shows the three types of pulse charging techniques. The rest and discharge phases aim to reduce the following: (a)the mechanical stress in electrode particles due to uneven insertion and extraction of lithium in the solid particles, (b) the possibility of electrochemical potential at anode becoming negative and concentration polarisation. Researches have shown other benefits, such as inhibition of dendrite formation in battery, better charge and discharge efficiency, and active material utilisation[56].

Works in literature have shown that application of high current when the battery is at a state of high open-circuit voltage (OCV) and high SoC accelerates the battery degradation due to increased intercalation of Li^+ ions in electrodes and side reactions in the surrounding region of electrodes in battery[14]. However, at the state of low OCV and SoC, the battery can be charged at high currents. Hence, Notten et al. proposed a charging technique called boost charging[33]. Boost charging is characterised by a high charge current (1C) for a short period leading to a fast charge up to one-third of the battery capacity. After that, conventional controlled low current CCCV is used to charge the remaining capacity. Although boost charging resulted in fast charge with controlled degradation, the implementation is a challenge because of the unknown high current that flows into the battery due to high voltage at the charger terminals. Moreover, the temperature rise and the degradation studies are not yet well discussed in the literature for boost charging. Compared to other charging techniques like CCCV, boost charging is able to input more charge in the battery when recorded in the initial fast charge period. However, the rise in battery temperature during boost charge was another challenge[32,33,53].

Numerous studies have shown a rise in temperature with an increase in the number of charge-discharge cycles. The temperature rise in the battery is due to an increase in the impedance or the chemical kinetics on the application of high current to charge or both[20]. Hence, considering the impact of temperature in ageing, Xiaosong analysed a new type of charging protocol, constant voltage constant temperature using the electro-thermal-ageing model. The analysis showed a tradeoff between charge time and the ageing of the battery. Constant temperature constant voltage (CTCV) charging protocol is another technique proposed considering the importance of temperature in the ageing of battery[23]. CTCV has simplicity in implementation and results in 20% faster charging when compared with CCCV.

Chen introduced sinusoidal ripple charging (SRC), claiming reduced charging time, charging efficiency and lifetime of battery with a controlled temperature rise of battery[57]. A challenge in using SRC for practical chargers is precise control in the magnitude and frequency of charging current. The frequency should be optimal to have a low impedance of the battery. Further, the magnitude of the ripple, which affects polarisation in battery and selection of components in the charger, need to be monitored[58–61]. Hence, a new power electronics converter topology for the charger and precise control of outputs (current and voltage) with the ability to reduce power quality for vehicle-to-grid issues is proposed in[60]. Further, suppression of dendrite growth in the battery is another benefit demonstrated in[62]. On the contrary, Bessman showed using experiments on prismatic cells and a physics-based model that the claimed benefits of SRC are not true as mentioned in literature[63].

In recent years, a new research direction has opened towards the model-based charging system. Information gathered from electrical and electrochemical modelling of batteries can be utilised to optimise the charging for a battery. The model-based charging technique uses electrical, electrochemical and thermal models and computes parameters for the battery[64–71]. The parameters computed using the electrical model include impedance and SoC. The electrochemical model computes SEI potential or thickness, active material concentration, and anode potential. Capacity, temperature and SoH are common to the model-based charging techniques. The works in this research directions also demonstrated a decrease in charge time and control of the rise in battery temperature. However, a few considered the effect of battery degradation during charging. Further, the advantage of model-based charging is demonstrated in simulation due to the requirements of multiple battery parameters and extensive computational cost.

The study on the parameter variations of Li-ion battery involves experimental procedures which requires enormous time and the use of precise measurement instruments. Mathematical models which capture various phenomenon within the battery are replacement for the experiments. Hence, mathematical models are widely proposed and used in the literature to design new battery or manage battery systems. Butler-Volmer equations and Nernst's theory are the earliest approaches to describe the physics in batteries. The Butler-Volmer equation relates the current density and the overpotential in batteries[72]. In contrast, Nernst's equation describes the electric potential of the electrode and electrical charge in the battery[73]. These equations were simple, but it was not sufficient to describe the complex physics of advanced Li-ion chemistries. Newman et al. developed the porous electrode theory, which became a standard mathematical model for Li-ion batteries. The model is popularly reported as Doyle-Fuller-Newman (DFN) model in literature[74,75]. The Butler-Volmer and Nernst equations use differential-algebraic equations, while the DFN model use partial differential equations. The equations of the DFN model are solved using a variety of numerical solving tools like control volumes, finite-difference methods, finite element methods, orthogonal collocation and others. The challenge in using DFN is the complexity to solve the equations even after using the listed variety of numerical solving tools.

Alternatively, equivalent circuit and simplified electrochemical models such as single-particle model and single-particle model with electrolyte are developed to meet the challenges of complexity, computational cost (speed and memory) and fast convergence to get results. Although alternative models solve the challenges, literature reports the requirement of correction factors to get appropriate results[76]. Hence, in this work DFN is selected to analyse the electrical, electrochemical, and mechanical parameters of the battery. The parameters of the battery used to simulate are given in Table S.3[18]. Apart from the parameters, various constant used in the simulation are also given in the table.

The governing equation of the DFN model is classified in three parts namely, charge conservation, molar conservation and electrochemical reactions. Each of them are discussed in detail in[76,77]. The governing equations are solved using Python Battery Mathematical Modelling (PyBaMM). The models of SEI formation, internal temperature variations and particle cracking were also incorporated[77–80]. These models are run for different types of charging and charging rates (0.3C to 5C) given in Table S.4 for 350 cycles. High performance computing platform-Param Ishan is used to simulate model.

References

[1] L. Lu, X. Han, J. Li, J. Hua, and M. Ouyang, "A review on the key issues for lithium-ion battery management in electric vehicles," *Journal of power sources*, vol. 226, pp. 272–288, 2013.

[2] A. Masias, J. Marcicki, and W. A. Paxton, "Opportunities and challenges of lithium ion batteries in automotive applications," *ACS Energy Letters*, vol. 6, no. 2, pp. 621–630, 2021.

[3] G. E. Blomgren, "The development and future of lithium ion batteries," *Journal of The Electrochemical Society*, vol. 164, no. 1, p. A5019, 2016.

[4] D. Kushnir, "lithium ion battery recycling technology 2015," *Current State and Future Prospects*, pp. 1–56, 2015.

[5] N. Nitta, F. Wu, J. T. Lee, and G. Yushin, "Li-ion battery materials: present and future," *Materials Today*, vol. 18, no. 5, pp. 252–264, 2015. [Online]. Available: https://www.sciencedirect.com/science/article/pii/S1369702114004118

[6] L. Ellingsen and C. Hung, "Research for tran committee-battery-powered electric vehicles: market development and lifecycle emissions," *STUDY, European Parliament, Directorate General for Internal Policies, Policy Department for Structural and Cohesion Policies, Transport and Tourism*, vol. 10, p. 944056, 2018.

[7] F. Conte, "Battery and battery management for hybrid electric vehicles: a review," *e & i Elektrotechnik und Informationstechnik*, vol. 123, no. 10, pp. 424–431, 2006.

[8] P. Keil, S. F. Schuster, J. Wilhelm, J. Travi, A. Hauser, R. C. Karl, and A. Jossen, "Calendar aging of lithium-ion batteries," *Journal of The Electrochemical Society*, vol. 163, no. 9, p. A1872, 2016.

[9] J. Vetter, P. Novák, M. R. Wagner, C. Veit, K.-C. Möller, J. Besenhard, M. Winter, M. Wohlfahrt-Mehrens, C. Vogler, and A. Hammouche, "Ageing mechanisms in lithium-ion batteries," *Journal of power sources*, vol. 147, no. 1-2, pp. 269–281, 2005.

[10] M. R. Palacín, "Understanding ageing in li-ion batteries: a chemical issue," *Chemical Society Reviews*, vol. 47, no. 13, pp. 4924–4933, 2018.

[11] X. Han, L. Lu, Y. Zheng, X. Feng, Z. Li, J. Li, and M. Ouyang, "A review on the key issues of the lithium ion battery degradation among the whole life cycle," *eTransportation*, vol. 1, p. 100005, 2019. [Online]. Available: https://www.sciencedirect.com/science/article/pii/S2590116819300050

[12] M. Kabir and D. E. Demirocak, "Degradation mechanisms in li-ion batteries: a state-of-the-art review," *International Journal of Energy Research*, vol. 41, no. 14, pp. 1963–1986, 2017.

[13] V. Etacheri, R. Marom, R. Elazari, G. Salitra, and D. Aurbach, "Challenges in the development of advanced li-ion batteries: a review," *Energy & Environmental Science*, vol. 4, no. 9, pp. 3243–3262, 2011.

[14] G. Sikha, B. N. Popov, and R. E. White, "Effect of porosity on the capacity fade of a lithium-ion battery: Theory," *Journal of the Electrochemical Society*, vol. 151, no. 7, p. A1104, 2004.

[15] Y. Zhang, C. Zhao, and Z. Guo, "Simulation of crack behavior of secondary particles in li-ion battery electrodes during lithiation/de-lithiation cycles," *International Journal of Mechanical Sciences*, vol. 155, pp. 178–186, 2019.

[16] P. Arora, R. E. White, and M. Doyle, "Capacity fade mechanisms and side reactions in lithium-ion batteries," *Journal of the Electrochemical Society*, vol. 145, no. 10, p. 3647, 1998.

[17] J. Liu, Q. Duan, M. Ma, C. Zhao, J. Sun, and Q. Wang, "Aging mechanisms and thermal stability of aged commercial 18650 lithium ion battery induced by slight overcharging cycling," *Journal of Power Sources*, vol. 445, p. 227263, 2020.

[18] P. Ramadass, B. Haran, P. M. Gomadam, R. White, and B. N. Popov, "Development of first principles capacity fade model for li-ion cells," *Journal of the Electrochemical Society*, vol. 151, no. 2, p. A196, 2004.

[19] D. Zhang, B. Haran, A. Durairajan, R. E. White, Y. Podrazhansky, and B. N. Popov, "Studies on capacity fade of lithium-ion batteries," *Journal of Power Sources*, vol. 91, no. 2, pp. 122–129, 2000.

[20] P. Ramadass, B. Haran, R. White, and B. N. Popov, "Capacity fade of sony 18650 cells cycled at elevated temperatures: Part i. cycling performance," *Journal of power sources*, vol. 112, no. 2, pp. 606–613, 2002.

[21] P. Keil and A. Jossen, "Charging protocols for lithium-ion batteries and their impact on cycle life—an experimental study with different 18650 high-power cells," *Journal of Energy Storage*, vol. 6, pp. 125–141, 2016.

[22] G. Sikha, P. Ramadass, B. Haran, R. E. White, and B. N. Popov, "Comparison of the capacity fade of sony us 18650 cells charged with different protocols," *Journal of power sources*, vol. 122, no. 1, pp. 67–76, 2003.

[23] L. Patnaik, A. Praneeth, and S. S. Williamson, "A closed-loop constant-temperature constant-voltage charging technique to reduce charge time of lithium-ion batteries," *IEEE Transactions on Industrial Electronics*, vol. 66, no. 2, pp. 1059–1067, 2018.

[24] B. Balagopal and M.-Y. Chow, "The physical manifestation of side reactions in the electrolyte of lithium-ion batteries and its impact on the terminal voltage response," *Batteries*, vol. 6, no. 4, p. 53, 2020.

[25] M. H.-M. Tang, "Side reactions in lithium-ion batteries," Ph.D. dissertation, UC Berkeley, 2012.

[26] R. Xiong, Y. Pan, W. Shen, H. Li, and F. Sun, "Lithium-ion battery aging mechanisms and diagnosis method for automotive applications: Recent advances and perspectives," *Renewable and Sustainable Energy Reviews*, vol. 131, p. 110048, 2020.

[27] K. Takahashi and V. Srinivasan, "Examination of graphite particle cracking as a failure mode in lithium-ion batteries: a model-experimental study," *Journal of The Electrochemical Society*, vol. 162, no. 4, p. A635, 2015.

[28] X. Zhang, A. M. Sastry, and W. Shyy, "Intercalation-induced stress and heat generation within single lithium-ion battery cathode particles," *Journal of The Electrochemical Society*, vol. 155, no. 7, p. A542, 2008.

[29] D. Lisbona and T. Snee, "A review of hazards associated with primary lithium and lithium-ion batteries," *Process Safety and Environmental Protection*, vol. 89, no. 6, pp. 434–442, 2011.

[30] S. Pelletier, O. Jabali, G. Laporte, and M. Veneroni, "Battery degradation and behaviour for electric vehicles: Review and numerical analyses of several models," *Transportation Research Part B: Methodological*, vol. 103, pp. 158–187, 2017.

[31] C. M. Snyder, "The rate depedency of li-ion battery degradation mechanisms." Sandia National Lab.(SNL-NM), Albuquerque, NM (United States), Tech. Rep., 2016.

[32] M. F. Hasan, C.-F. Chen, C. E. Shaffer, and P. P. Mukherjee, "Analysis of the implications of rapid charging on lithium-ion battery performance," *Journal of the Electrochemical Society*, vol. 162, no. 7, p. A1382, 2015.

[33] P. H. Notten, J. O. het Veld, and J. Van Beek, "Boostcharging li-ion batteries: A challenging new charging concept," *Journal of Power Sources*, vol. 145, no. 1, pp. 89–94, 2005.

[34] D. H. Doughty and C. C. Crafts, "Freedomcar: electrical energy storage system abuse test manual for electric and hybrid electric vehicle applications." Sandia National Laboratories, Tech. Rep., 2006.

[35] X. Zhou, J. Huang, Z. Pan, and M. Ouyang, "Impedance characterization of lithium-ion batteries aging under high-temperature cycling: Importance of electrolyte-phase diffusion," *Journal of Power Sources*, vol. 426, pp. 216–222, 2019.

[36] A. Barré, B. Deguilhem, S. Grolleau, M. Gérard, F. Suard, and D. Riu, "A review on lithium-ion battery ageing mechanisms and estimations for automotive applications," *Journal of Power Sources*, vol. 241, pp. 680–689, 2013.

[37] A. Andersson and K. Edström, "Chemical composition and morphology of the elevated temperature sei on graphite," *Journal of the Electrochemical Society*, vol. 148, no. 10, p. A1100, 2001.

[38] M. Richard and J. Dahn, "Accelerating rate calorimetry study on the thermal stability of lithium intercalated graphite in electrolyte. i. experimental," *Journal of The Electrochemical Society*, vol. 146, no. 6, p. 2068, 1999.

[39] ——, "Accelerating rate calorimetry study on the thermal stability of lithium intercalated graphite in electrolyte. ii. modeling the results and predicting differential scanning calorimeter curves," *Journal of The Electrochemical Society*, vol. 146, no. 6, p. 2078, 1999.

[40] H. Maleki, G. Deng, A. Anani, and J. Howard, "Thermal stability studies of li-ion cells and components," *Journal of The electrochemical society*, vol. 146, no. 9, p. 3224, 1999.

[41] D. MacNeil, D. Larcher, and J. Dahn, "Comparison of the reactivity of various carbon electrode materials with electrolyte at elevated temperature," *Journal of the electrochemical society*, vol. 146, no. 10, p. 3596, 1999.

[42] P. Arora, M. Doyle, and R. E. White, "Mathematical modeling of the lithium deposition overcharge reaction in lithium-ion batteries using carbon-based negative electrodes," *Journal of The Electrochemical Society*, vol. 146, no. 10, p. 3543, 1999.

[43] C.-K. Huang, J. Sakamoto, J. Wolfenstine, and S. Surampudi, "The limits of low-temperature performance of li-ion cells," *Journal of the Electrochemical Society*, vol. 147, no. 8, p. 2893, 2000.

[44] A. Pesaran, S. Santhanagopalan, and G. Kim, "Addressing the impact of temperature extremes on large format li-ion batteries for vehicle applications (presentation)," National Renewable Energy Lab.(NREL), Golden, CO (United States), Tech. Rep., 2013.

[45] L.-R. Chen, "A design of an optimal battery pulse charge system by frequency-varied technique," *IEEE Transactions on Industrial Electronics*, vol. 54, no. 1, pp. 398–405, 2007.

[46] B. Sah, P. Kumar, R. Rayudu, S. K. Bose, and K. P. Inala, "Impact of sampling in the operation of vehicle to grid and its mitigation," *IEEE Transactions on Industrial Informatics*, vol. 15, no. 7, pp. 3923–3933, 2018.

[47] B. Sah, P. Kumar, and S. K. Bose, "A fuzzy logic and artificial neural network-based intelligent controller for a vehicle-to-grid system," *IEEE Systems Journal*, 2020.

[48] M. Muratori, "Impact of uncoordinated plug-in electric vehicle charging on residential power demand," *Nature Energy*, vol. 3, no. 3, pp. 193–201, 2018.

[49] A. Raj, M.-T. F. Rodrigues, and D. P. Abraham, "Rate-dependent aging resulting from fast charging of li-ion cells," *Journal of The Electrochemical Society*, vol. 167, no. 12, p. 120517, 2020.

[50] S. S. Zhang, "The effect of the charging protocol on the cycle life of a li-ion battery," *Journal of power sources*, vol. 161, no. 2, pp. 1385–1391, 2006.

[51] A. Tomaszewska, Z. Chu, X. Feng, S. O'Kane, X. Liu, J. Chen, C. Ji, E. Endler, R. Li, L. Liu, Y. Li, S. Zheng, S. Vetterlein, M. Gao, J. Du, M. Parkes, M. Ouyang, M. Marinescu, G. Offer, and B. Wu, "Lithium-ion battery fast charging: A review," *eTransportation*, vol. 1, p. 100011, 2019. [Online]. Available: https://www.sciencedirect.com/science/article/pii/S2590116819300116

[52] J. Li, E. Murphy, J. Winnick, and P. A. Kohl, "The effects of pulse charging on cycling characteristics of commercial lithium-ion batteries," *Journal of Power Sources*, vol. 102, no. 1-2, pp. 302–309, 2001.

[53] S. Li, Q. Wu, D. Zhang, Z. Liu, Y. He, Z. L. Wang, and C. Sun, "Effects of pulse charging on the performances of lithium-ion batteries," *Nano Energy*, vol. 56, pp. 555–562, 2019.

[54] F. Savoye, P. Venet, M. Millet, and J. Groot, "Impact of periodic current pulses on li-ion battery performance," *IEEE Transactions on Industrial Electronics*, vol. 59, no. 9, pp. 3481–3488, 2011.

[55] H. Lv, X. Huang, and Y. Liu, "Analysis on pulse charging–discharging strategies for improving capacity retention rates of lithium-ion batteries," *Ionics*, pp. 1–22, 2020.

[56] S. Li, Q. Wu, D. Zhang, Z. Liu, Y. He, Z. L. Wang, and C. Sun, "Effects of pulse charging on the performances of lithium-ion batteries," *Nano Energy*, vol. 56, pp. 555–562, 2019. [Online]. Available: https://www.sciencedirect.com/science/article/pii/S2211285518308826

[57] L.-R. Chen, S.-L. Wu, D.-T. Shieh, and T.-R. Chen, "Sinusoidal-ripple-current charging strategy and optimal charging frequency study for li-ion batteries," *IEEE Transactions on Industrial Electronics*, vol. 60, no. 1, pp. 88–97, 2012.

[58] Y. Lee and S. Park, "Electrochemical state-based sinusoidal ripple current charging control," *IEEE Transactions on Power Electronics*, vol. 30, no. 8, pp. 4232–4243, 2015.

[59] J. Chen, Y. Lee, and S. Park, "Adaptive pi gain control to realize sinusoidal ripple current charging," in *2015 9th International Conference on Power Electronics and ECCE Asia (ICPE-ECCE Asia)*, 2015, pp. 2582–2589.

[60] M. Bayati, M. Abedi, G. B. Gharehpetian, and M. Farahmandrad, "Sinusoidal-ripple current control in battery charger of electric vehicles," *IEEE Transactions on Vehicular Technology*, vol. 69, no. 7, pp. 7201–7210, 2020.

[61] H. Vazini, "Sinusoidal charging of li-ion battery based on frequency detection algorithm by pole placement control method," *IET Power Electronics*, vol. 12, pp. 421–429(8), March 2019.

[62] Z. Zhang, Z. L. Wang, and X. Lu, "Suppressing lithium dendrite growth via sinusoidal ripple current produced by triboelectric nanogenerators," *Advanced Energy Materials*, vol. 9, no. 20, p. 1900487, 2019. [Online]. Available: https://onlinelibrary.wiley.com/doi/abs/10.1002/aenm.201900487

[63] A. Bessman, R. Soares, S. Vadivelu, O. Wallmark, P. Svens, H. Ekström, and G. Lindbergh, "Challenging sinusoidal ripple-current charging of lithium-ion batteries," *IEEE Transactions on Industrial Electronics*, vol. 65, no. 6, pp. 4750–4757, 2018.

[64] X. Lin, X. Hao, Z. Liu, and W. Jia, "Health conscious fast charging of li-ion batteries via a single particle model with aging mechanisms," *Journal of Power Sources*, vol. 400, pp. 305–316, 2018.

[65] H. Perez, S. Dey, X. Hu, and S. Moura, "Optimal charging of li-ion batteries via a single particle model with electrolyte and thermal dynamics," *Journal of The Electrochemical Society*, vol. 164, no. 7, p. A1679, 2017.

[66] S. Pramanik and S. Anwar, "Electrochemical model based charge optimization for lithium-ion batteries," *Journal of Power Sources*, vol. 313, pp. 164–177, 2016.

[67] T. Waldmann, M. Kasper, and M. Wohlfahrt-Mehrens, "Optimization of charging strategy by prevention of lithium deposition on anodes in high-energy lithium-ion batteries–electrochemical experiments," *Electrochimica Acta*, vol. 178, pp. 525–532, 2015.

[68] F. B. Spingler, W. Wittmann, J. Sturm, B. Rieger, and A. Jossen, "Optimum fast charging of lithium-ion pouch cells based on local volume expansion criteria," *Journal of Power Sources*, vol. 393, pp. 152–160, 2018.

[69] S. Schindler, M. Bauer, H. Cheetamun, and M. A. Danzer, "Fast charging of lithium-ion cells: identification of aging-minimal current profiles using a design of experiment approach and a mechanistic degradation analysis," *Journal of Energy Storage*, vol. 19, pp. 364–378, 2018.

[70] C. Zou, X. Hu, Z. Wei, T. Wik, and B. Egardt, "Electrochemical estimation and control for lithium-ion battery health-aware fast charging," *IEEE Transactions on Industrial Electronics*, vol. 65, no. 8, pp. 6635–6645, 2017.

[71] M. Song and S.-Y. Choe, "Fast and safe charging method suppressing side reaction and lithium deposition reaction in lithium ion battery," *Journal of Power Sources*, vol. 436, p. 226835, 2019.

[72] E. J. Dickinson and A. J. Wain, "The butler-volmer equation in electrochemical theory: Origins, value, and practical application," *Journal of Electroanalytical Chemistry*, vol. 872, p. 114145, 2020, dr. Richard Compton 65th birthday Special issue. [Online]. Available: https://www.sciencedirect.com/science/article/pii/S1572665720303283

[73] A. Seaman, T.-S. Dao, and J. McPhee, "A survey of mathematics-based equivalent-circuit and electrochemical battery models for hybrid and electric vehicle simulation," *Journal of Power Sources*, vol. 256, pp. 410–423, 2014. [Online]. Available: https://www.sciencedirect.com/science/article/pii/S0378775314000810

[74] M. Doyle, T. F. Fuller, and J. Newman, "Modeling of galvanostatic charge and discharge of the lithium/polymer/insertion cell," *Journal of the Electrochemical society*, vol. 140, no. 6, p. 1526, 1993.

[75] C. M. Doyle, "Design and simulation of lithium rechargeable batteries," 1995.

[76] S. G. Marquis, V. Sulzer, R. Timms, C. P. Please, and S. J. Chapman, "An asymptotic derivation of a single particle model with electrolyte," *Journal of The Electrochemical Society*, vol. 166, no. 15, p. A3693, 2019.

[77] R. Timms, S. G. Marquis, V. Sulzer, C. P. Please, and S. J. Chapman, "Asymptotic reduction of a lithium-ion pouch cell model," *SIAM Journal on Applied Mathematics*, vol. 81, no. 3, pp. 765–788, 2021.

[78] R. Deshpande, M. Verbrugge, Y.-T. Cheng, J. Wang, and P. Liu, "Battery cycle life prediction with coupled chemical degradation and fatigue mechanics," *Journal of the Electrochemical Society*, vol. 159, no. 10, p. A1730, 2012.

[79] W. Ai, L. Kraft, J. Sturm, A. Jossen, and B. Wu, "Electrochemical thermal-mechanical modelling of stress inhomogeneity in lithium-ion pouch cells," *Journal of The Electrochemical Society*, vol. 167, no. 1, p. 013512, 2019.

[80] X.-G. Yang, Y. Leng, G. Zhang, S. Ge, and C.-Y. Wang, "Modeling of lithium plating induced aging of lithium-ion batteries: Transition from linear to nonlinear aging," *Journal of Power Sources*, vol. 360, pp. 28–40, 2017.

[81] S. S. Choi and H. S. Lim, "Factors that affect cycle-life and possible degradation mechanisms of a li-ion cell based on licoo2," *Journal of Power Sources*, vol. 111, no. 1, pp. 130–136, 2002. [Online]. Available: https://www.sciencedirect.com/science/article/pii/S0378775302003051

[82] Z. Yan and M. Obrovac, "Selecting inactive materials with low electrolyte reactivity for lithium-ion cells," *Journal of Power Sources*, vol. 397, pp. 374–381, 2018. [Online]. Available: https://www.sciencedirect.com/science/article/pii/S037877531830750X

[83] C. J. Orendorff, G. Nagasubramanian, T. N. Lambert, K. R. Fenton, C. A. Apblett, C. R. Shaddix, M. Geier, and E. P. Roth, "Advanced inactive materials for improved lithium-ion battery safety," *Sandia Report SAND*, vol. 9186, p. 2012, 2012.

[84] E. Foreman, W. Zakri, M. Hossein Sanatimoghaddam, A. Modjtahedi, S. Pathak, A. G. Kashkooli, N. G. Garafolo, and S. Farhad, "A review of inactive materials and components of flexible lithium-ion batteries," *Advanced Sustainable Systems*, vol. 1, no. 11, p. 1700061, 2017.

[85] Y. Jeon, H. K. Noh, and H.-K. Song, "A lithium-ion battery using partially lithiated graphite anode and amphi-redox $limn_2o_4$ cathode," *Scientific reports*, vol. 7, no. 1, pp. 1–9, 2017.

[86] T. R. Ferguson, "Lithium-ion battery modeling using non-equilibrium thermodynamics," Ph.D. dissertation, Massachusetts Institute of Technology, 2014.

[87] T.-T. Nguyen, A. Demortière, B. Fleutot, B. Delobel, C. Delacourt, and S. J. Cooper, "The electrode tortuosity factor: why the conventional tortuosity factor is not well suited for quantifying transport in porous li-ion battery electrodes and what to use instead," *npj Computational Materials*, vol. 6, no. 1, pp. 1–12, 2020.

[88] J. Landesfeind, J. Hattendorff, A. Ehrl, W. A. Wall, and H. A. Gasteiger, "Tortuosity determination of battery electrodes and separators by impedance spectroscopy," *Journal of The Electrochemical Society*, vol. 163, no. 7, p. A1373, 2016.

[89] B. Tjaden, D. J. Brett, and P. R. Shearing, "Tortuosity in electrochemical devices: a review of calculation approaches," *International Materials Reviews*, vol. 63, no. 2, pp. 47–67, 2018.

Acknowledgements: This work is supported by the Electric Mobility lab of the Department of Electronics and Electrical Engineering, Indian Institute of Technology Guwahati. The author would like to extend their thanks to the developers of Python Battery Mathematical Modelling (PyBaMM), specifically Dr Valentin Sulzer, for his support while preparing models and codes for implementing charging techniques.

Author Contributions: Bikash Sah and Praveen Kumar conceived and designed the research. Bikash Sah acquired the data, implemented the physics-based model of Li-ion battery, integrated the models of battery degradation, designed types of charging techniques, performed the data analysis and visualisation. Both the authors contributed to discussing results and writing the manuscript.

Competing Interests: The authors declare that they have no competing interests.

Correspondence: Correspondence and request for any details in manuscript can be made to Bikash Sah (bikash.2015@iitg.ac.in)

Additional information: Supplementary information including plots, explanations and data are attached.

Supplementary results and discussions

An Insight into the Battery Degradation and a Proposal for a Battery Friendly Charging Technique

Bikash Sah, Praveen Kumar
Department of Electronics and Electrical Engineering,
Indian Institute of Technology Guwahati, Assam, 781039, India

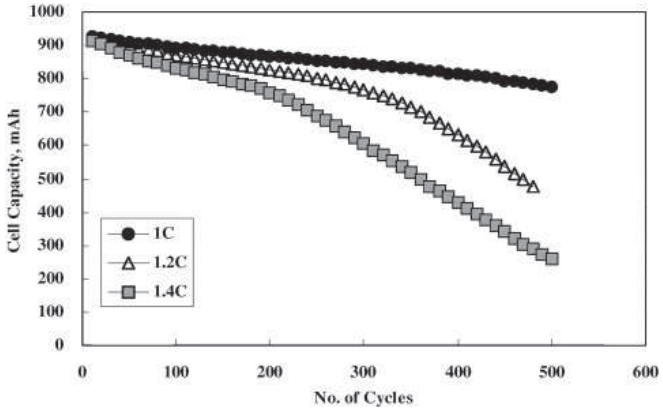

Figure S.1: The acceleration of capacity fade with increase in charging rate as described in[81]

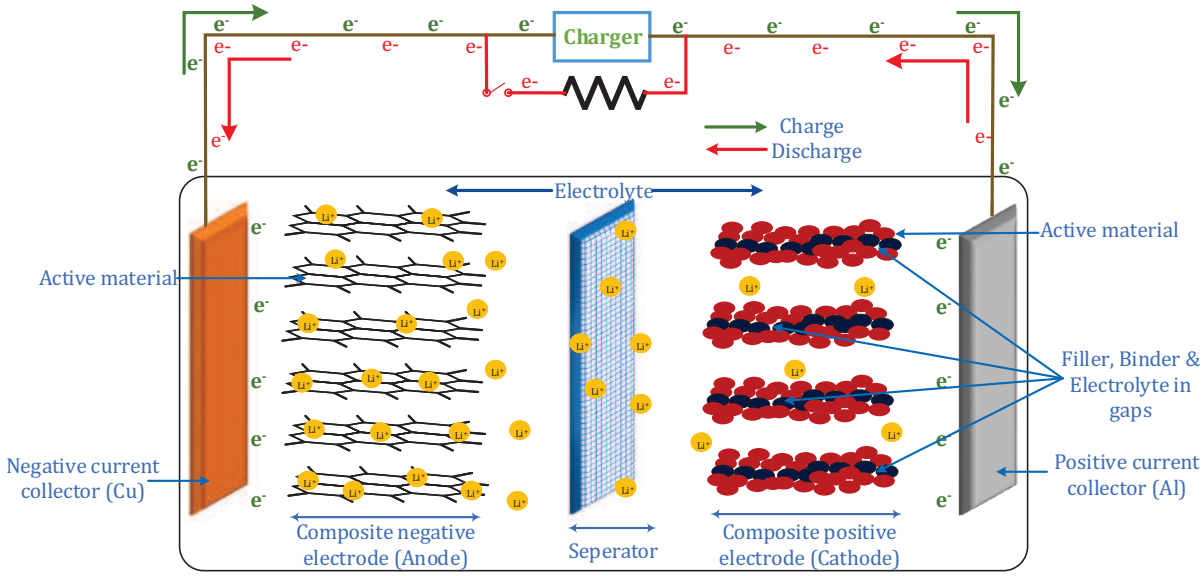

Figure S.2: The model of the battery with all components depicting the process of charging and discharging using the direction of flow of electrons. The arrows and ions in red depicts the process of discharge while the green depicts charging process. The electrons flow via the connecting wires and the positive ions diffuse to either electrodes (positive or negative) depending on the process of charging and discharging via electrolyte.

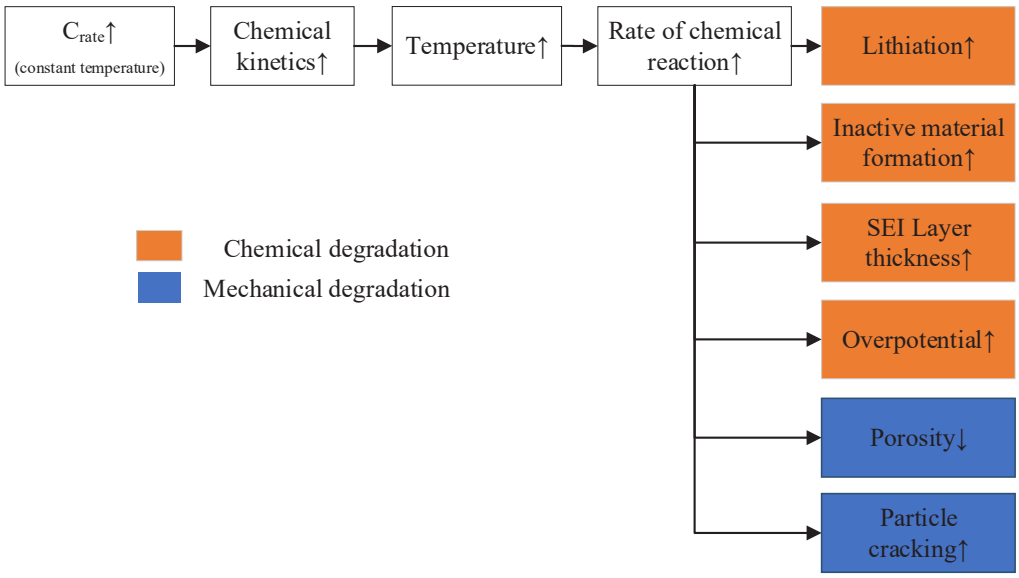

Figure S.3: The figure shows a list of parameters and their classification as chemical and mechanical. The chemical are marked in orange while the blue represents the mechanical parameters. Adjacent to each parameters, the arrow shows its variation when there is increase in C_{rate}. The figure try to relate different types of parameters and convey a possible sequence of events with change in C_{rate}.

Table S.1: The different types of parameters studied or used in models reported to date are presented in this table. The electrical model requires least number of parameters to be modelled but help in deriving required health status. The electrochemical model is computationally expensive and demands numerous parameters which are either available only with the manufacturer or determined using sophisticated test and equipments. The mechanical model is also similar to the electrochemical model but the governing equations used are different. Both electrochemical and mechanical model help in determining the health of the battery.

Charging technique	**Electrical**	**Electrochemical**	**Mechanical**
CCCV	Capacity, impedance, efficiency (charge and energy), OCV, SoC, and SoH	Electrode potential, side reaction rate, active material concentration, Lithium loss, SEI (thickness, density, resistance), and exchange current density.	Porosity, stress, expansion (cell width and length), structural disordering
Pulse charging	Capacity, impedance, SoC, efficiency (charge and energy)	Li-loss, surface concentration, transfer reaction	Structuring disordering and porosity
Model based	Impedance, differential voltage, SoC, SoH, ohmic loss, capacity, energy	Polarization voltage, SEI (thickness and potential), electrode potential, Li concentration, active material concentration	
Boost charging	Capacity, charge efficiency	Concentration (electrolyte, surface) transfer reaction	Porosity
Temperature based	SoC, impedance, capacity, SoH and end-of-life		

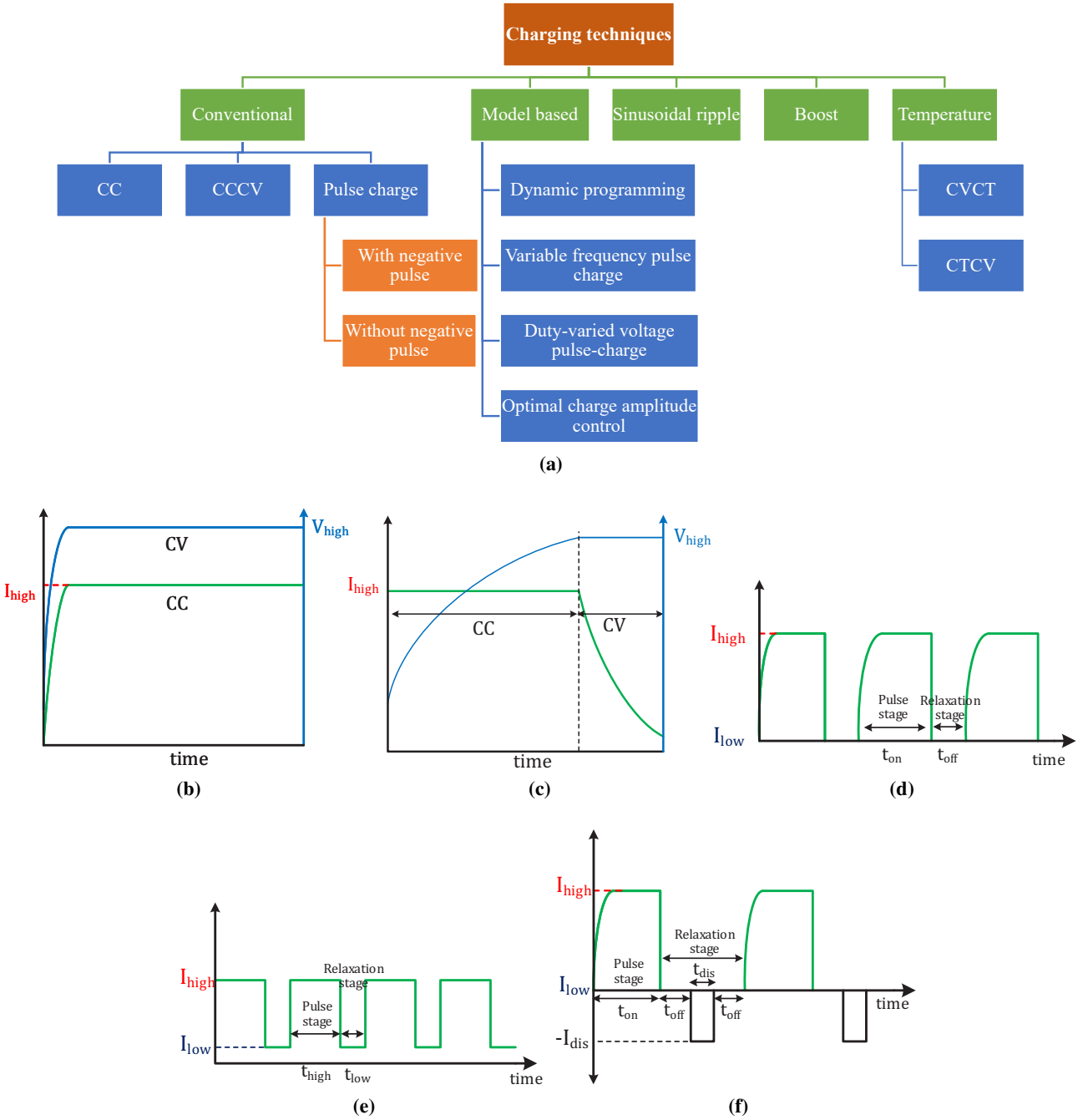

Figure S.4: Types of charging techniques reported in literature and a few typical current and voltage waveforms; (a) All the types of charing reported in the literature are extensively reviewed and classified appropriately. (b) The current waveforms in constant current (CC) and voltage waveform in constant voltage (CV) charging technique are shown, (c) The variation in current and voltage waveforms in constant current constant voltage (CCCV) is shown. When current is constant, the voltage varies and vice-versa, (d) The current waveform in pulse charging without discharge with pulse stage and relaxation stage is shown, (e) The current waveform in pulse charging with different current amplitude stage is shown. The current is never equal to zero in this charging technique. (f) The current waveform in pulse charging with short discharge pulse is shown. It comprises of pulse stage and relaxation stage, where relaxation stage is further having off period and discharge period.

Inactive material concentration

Li-ion batteries have active and inactive materials. Those materials that contribute to the energy storage process, such as storing lithium, are the active materials. The inactive materials include separator, binders, current collectors, electrolyte, additives and packaging components[82,83]. These inactive materials constitute almost 60% of the battery weight and hence, are a crucial parameter affecting the battery energy and power density[84]. The concentration of inactive materials keeps increasing with the age of the battery. The side reactions in the battery are a major cause supporting the conversion of active materials to inactive[16,80,82].

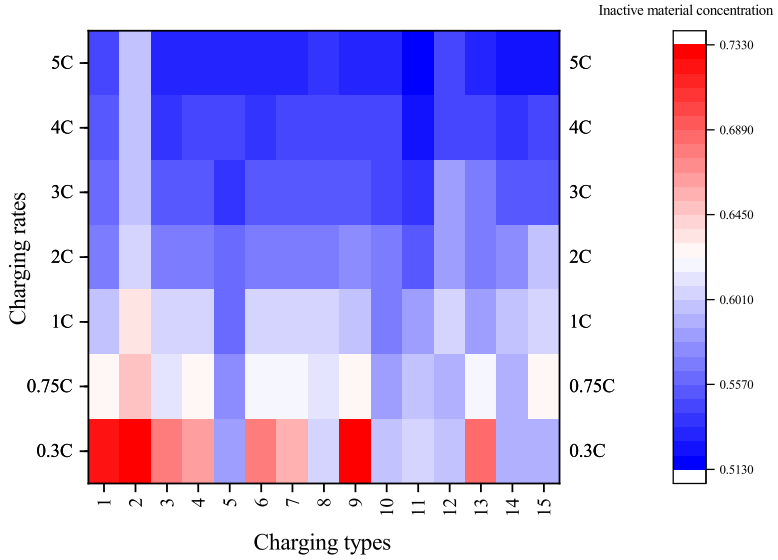

Figure S.5: The variation of X-averaged negative electrode inactive material volume fraction when the elected battery us charged using different types of charging techniques at different C_{rate} is shown. The lower charging rates results in maximum formation of inactive materials because chemical degradation dominates at lower C_{rate}.

Fig. S.5 shows the formation of inactive material in the battery when different types of charging are used at different charging rates. The inactive material formation is the highest at lower charging rates. The charging technique 1 (CC), 2 (CCCV) and 9 (pulse charge with discharge) shows the highest concentration of inactive material at the end of 350 cycles of charge and discharge at low discharging rates. With an increase in the charging rates, the amount of inactive material concentration reduced. The reduction in the formation of inactive material is related to two primary reasons: i) the battery reaches the cutoff potential faster because of the increased overpotential, and ii) the time to charge is reduced. The first reason is, a higher C_{rate} leads to an increase in chemical kinetics, charge transfer via diffusion and change in equilibrium potential. Since the overpotential is high, the cutoff voltage is reached faster, and the battery is considered to be charged. A larger time frame to charge at a slower C_{rate} leads to a larger time for side reactions.. Hence, the concentration of inactive materials is higher at slow C_{rate}.

CCCV and variants of pulse charging have shown reasonable changes in the concentration of inactive material formation. During CCCV, although the battery is charged at high currents during initial states, the charging end with a reduction in the C_{rate} or fall of charging current to 50 mA during CV mode. Hence, CCCV is the only technique in which there is the least variation of the concentration of inactive material followed by the pulse charging with discharge (charging type 12 and 13). Fig. S.5 shows the impact of the duty cycle, rest time and the amplitude of discharge pulse in different variants of pulse charging. The rest period during the pulse charge provides a settling time to the batteries. During the settling time, the increase in the chemical kinetics, charge transfer rate, and change in equilibrium potential is reduced or halted. Hence, the formation of inactive material is also less when compared to CC and CCCV. However, there are variations due to the parameters of the pulses. The interpretation of the concentration of inactive material for pulse charging without discharge is shown in charging type 3 to 8. The decrease in the concentration of inactive material is seen with a reduction of the t_{on}. For a higher t_{on}, the charging technique tends to behave like CC or CCCV; hence, a similar concentration is seen, although it is less than CC and CCCV. The t_{off} also impacts the formation of inactive materials. A reduction in the t_{off} leads to a reduction in the formation of inactive material. In general, a reduced t_{on} and t_{off} reduces the increase in the concentration of inactive material volume concentration.

The pulse charging with discharge leads to the least increase in the concentration of inactive material compared to CC, CCCV and pulse charge without discharge. Charge type 9 to 15 in Fig. S.5 shows the variation of the concentration of inactive material. The charge type 9, 10 and 11 are having a reduction t_{on} for a constant t_{off} and discharge time, resulting in reduced inactive material concentration. The results obtained follows a similar trend as observed in pulse charging without discharge. Further investigation on the impact of discharge pulse is studied by changing the amplitude. For simulations in which the amplitude of discharge current is equal to average current, but the on-time varies from highest to lowest (charge type 9, 10 and 11), the inactive material concentration is least for the smallest t_{on}. When the amplitude of discharge current is reduced to half of the average current, higher on-time resulted in the formation of less inactive material. In contrast, when the amplitude of discharge pulse is double the average current, inactive material volume concentration is more for a higher on-time. Hence, for pulse charging with discharge, with charge type in which the amplitude of discharge current equals the average current, and have least on-time results in the formation of least inactive material. The battery discharge process also renders a similar change in the equilibrium potential of the reactions in the batteries. Hence, an increase in the discharge pulse leads to a rise in the formation of inactive materials.

Reaction overpotential

The deviation of the battery potential from the electrode equilibrium potential to meet the requirements of current during charge or discharge is commonly called overpotential. A simplistic example of overpotential can be visualised by observing the increase in the terminal voltage of a battery when a charger is connected to it after allowing it to rest for an hour or more. Hence, a higher charge or discharge current will lead to an increase in the overpotential of the battery. Different types of overpotential are described in the literature. Those include thermodynamic, charge-transfer, ohmic and concentration overpotential. Splitting the overall overpotential is not done in this work. The literature describes that an increase in the SEI layer thickness (ohmic overpotential) add to the increase in the overpotential[31].

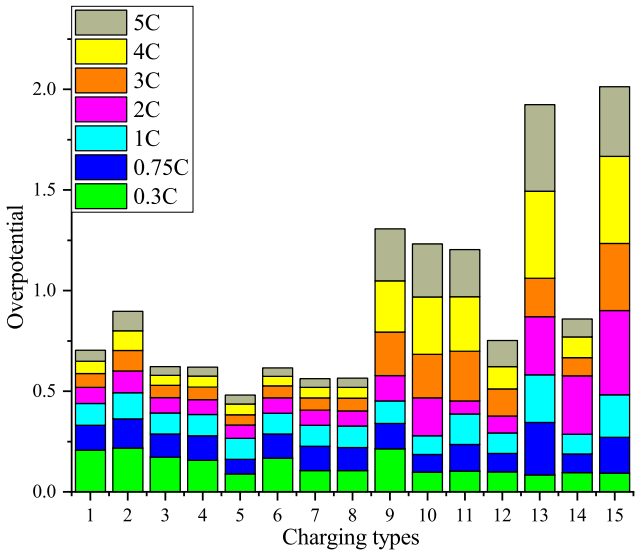

Figure S.6: The variation of X-averaged negative electrode reaction overpotential [V] when the battery is charged using different charging techniques at different C_{rate} is shown. The overpotential is higher at lower C_{rate} as the inactive material formation and SEI thickness is more.

Fig.S.6 shows the changes in the overpotential with an increase in the charging rates and change in the charging types. During CC and CCCV, the highest overpotential is seen during low C_{rate}. Since at low C_{rate}, the SEI formed is stable and thick, the ohmic overpotential due to SEI layer formation is dominant. Further, CCCV have higher overpotential when compared to CC, which is similar to the SEI layer thickness. Moving right in Fig.S.6, the variation of overpotential when variants of pulse charging are done is described. The rise in the overpotential is the least in CT5, which is attributed to SEI layer formation. With the decrease in t_{on} and t_{off}, the rise in overpotential decreases. The rest period in the pulse charge provided time to settle. Hence, the overpotential due to thermodynamics, charge transfer, and concentration reduces. Further, the growth of the SEI layer is also constrained due to the least deviation from equilibrium potential.

The pulse charging without discharge is found to reduce the rise in the overpotential. However, when the pulse charging with discharge is observed, a sudden increase in the overpotential is visible. Although the rise in the overpotential follows the trend of decreasing t_{on}, the SEI layer thickness is not the highest compared to Fig. 1a. Hence, in pulse charge with discharge, it is not the ohmic overpotential that dominates; it is the thermodynamics and the charge transfer overpotential that dominates. The claim is corroborated by the rise in cell temperature as seen in Fig. 1c. The charge transfer overpotential increases with an increase in the C_{rate}. Hence, with an increase in the amplitude of the discharge pulse, from half of the average charging current to double the charge current, the overpotential rises. Both thermodynamic and charge transfer overpotential dominates the rise in overpotential when pulse charging with discharge is performed with a higher amplitude discharge pulse. CT5 and CT 8 resulted in the best charging types when the increase in overpotential is accounted for.

Extent of lithiation

Lithiation is the intercalation of Li-ions in the negative electrode during charging. The extent of lithiation happening prominently impacts the capacity of the battery during charging. The formation cycle, which is done after the manufacturing of the battery, involves the process of prelithiate anode, which is also accompanied by SEI layer formation and a rise in overpotential during formation. Hence, the extent of lithiation is also related to SEI layer thickness, and overpotential[85]. Fig. S.7 shows the variation of lithiation at different charging techniques and rate.

The change in the extent of lithiation in CCCV is the least for different charging rates. A larger impact of C_{rate} is seen in CC. The process of lithiation is dependant on the ease to intercalate in the electrodes. The ease to intercalate further depends on the diameter of the pores. With the growth of the SEI layer, the diameter decreases and add resistance to the diffusion of ions. Hence, lithiation reduces with the ageing of the battery. At the lower C_{rate}, the SEI layer formed is thick and stable; hence, lithiation reduces.

On the contrary, although the SEI layer is less thick than the lower C_{rate}, the lithiation is less in the higher C_{rate}. Hence, there are other factors also that impacts the extent of lithiation. The higher C_{rate} leads to an increase in the chemical kinetics in the

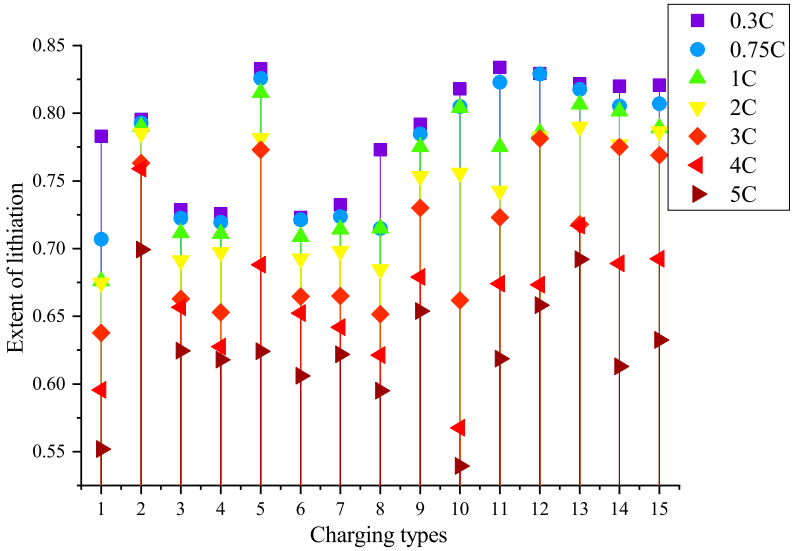

Figure S.7: The X-averaged negative electrode extent of lithiation for different types of charging and at different C_{rate} is shown. Lower C_{rate} results in better lithiation while higher C_{rate} reduces it. A better lithiation is related to overpotential and the chemical kinetics which impact the settlement of ions in electrodes.

battery. The equilibrium potential and overpotential also increases with an increase in the cell temperature. The overall change in the battery makes does not allow the Li-ion to settle in and stimulate various side reactions.

A few patterns of pulse charging shows better results when compared to conventional CC and CCCV. The variation of t_{on} and t_{off} shows similar changes in the variation of extent of lithiation. A decrease in the t_{on} and t_{off} leads to better lithiation. A larger t_{on} allows accumulative growth of SEI layer and cell temperature, and the t_{off} helps to settle the processes in the battery. A reduction in t_{on} time ensures a reduction in the accumulative growth of the SEI layer and temperature. The pulse charging with discharge good results in low charging rates, but the extent of lithiation reduced drastically at higher charging rates. The decrease in t_{on} is visible here as well, with improvement in the extent of lithiation. The amplitude of discharge pulse also impacts the lithiation, but visible changes are seen only at higher C_{rate}. At higher C_{rate}, the impact of SEI layer thickness and the processes leading to an increase in temperature dominates convolutes. However, the impact of the SEI layer is dominant only at low C_{rate}.

Porosity

The porosity of the electrodes is an important parameter that impacts the capacity of the Li-ion battery. The porosity of pores in the electrode is varied with the deposition of inactive materials, which is the SEI layer. With an increase in the thickness of the SEI layer, the pores get clogged, leading to a reduction in the intercalation reactions, as discussed in previous subsections[14]. Hence, the porosity also varies similarly as the inactive material, and SEI layer thickness varies. Fig. S.10b shows the variation of porosity of the negative electrode after 350 charge-discharge cycles. The porosity is the least in the case of CCCV and CC, followed by CT9. The variation in porosity in Fig. S.10b demonstrates that change in charging types have an impact on the performance of the battery, especially when looked into the variants of pulse charging.

The porosity impacts from the t_{on} and t_{off} for pulse charge without discharge. It is observed that for a lower value of on-time, the impact on the porosity is least and retain a higher value. A lower off-time too have a similar impact on the porosity. The charge type 5 shows the least variation in the porosity for different charge rates. With an increase in the C_{rate}, the change in the value of porosity is reduced. In contrast, a lower charging rate leads to a higher reduction of porosity with an increase in the number of cycles. As described in previous subsections, the SEI layer formed is thicker and stable at lower charging rates. Hence, porosity is reduced drastically, and the impact of pulse charging is also negligible. The pulse charging without discharge is capable of controlling the reduction in the porosity of the negative electrode. However, pulse charge with the discharge has shown similar benefits when the variation of t_{on} and t_{off} is investigated.

The variation of pulse charging with discharge is shown in charge type 9 to 15. The change in the porosity is reduced with the use of pulse charge with discharge because of the reduction in the SEI layer thickness as shown in Fig. 1a. The decrease in the t_{on} in this technique also impacts the porosity. For a higher value of on-time, the change in the porosity is greater at lower charging rates. For higher charging rates, the change in porosity is the least. The charge types- 9, 10, and 11 shows a reduction in the change in the porosity because of the reduction in t_{on}. The reduction in t_{on} stops a consistent rise in the rate of side reactions, and the t_{off} allows to settle processes. The amplitude of the discharge pulse also impacts the change in the porosity of the electrodes. For cases where the amplitude of discharge pulse is equal to the average current, the difference in porosity is with the reduction in t_{on}, the change in the porosity reduces. On the contrary, a more significant change in porosity is found when the amplitude of discharge current is equal to half of the average current.

A larger difference in porosity is observed for case the amplitude of discharge current is double the average current. The change in the porosity is related to the equilibrium potential, which on the increase in the magnitude, fall below the stability limits of the electrolyte leading to SEI formation. The rest period after the discharge pulse helps to stabilise the SEI layer. Hence, in the case of low C_{rate}, which also generates a stable SEI layer, the larger reduction in porosity is visible even when pulse charging with

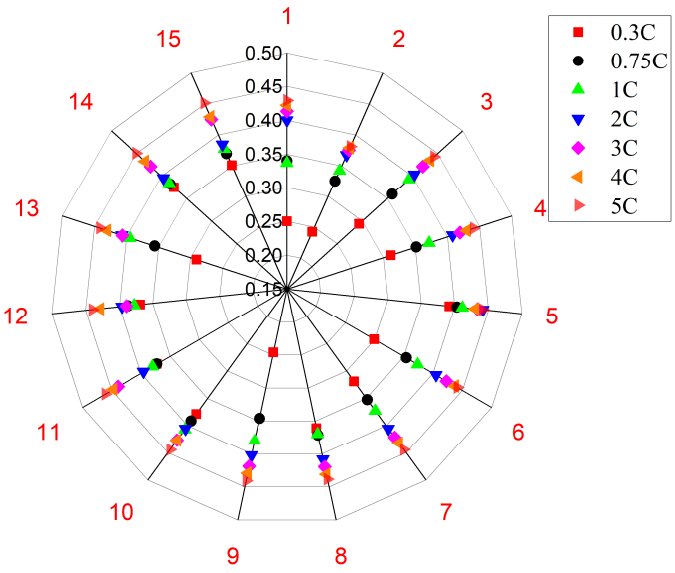

Figure S.8: The X-averaged negative electrode porosity for different types of charging and at different C_{rate} is shown. The porosity depends on the SEI layer thickness over particles in electrodes. Hence, at lower C_{rate}, when SEI layer thickness increases, the porosity of the electrodes is also reduces.

discharge is used.

Tortuosity

Tortuosity is an important factor relating to the mass and charge transport in an electrochemical device[86]. Although this factor plays a major role in the fast charging of batteries, it has not been widely discussed in works dealing with the capacity fade of batteries. Tortuosity is a microstructural characteristic that defines the ease of flow of ions during charging and discharging[87–89]. However, tortuosity should not be misunderstood with the geometric property of microstructure rather interpreted as the effective diffusibility of mass in a porous object[86]. A higher value of tortuosity infers that the travel path through the porous structure is not smooth or short for the charge. Hence, the lower the value of tortuosity, the better the charge and mass transport in the battery's electrodes[89].

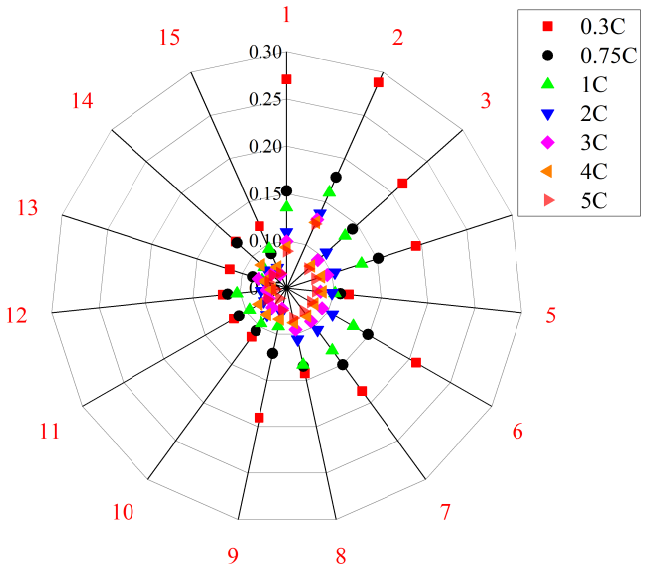

Figure S.9: The X-averaged negative electrode tortuosity for different types of charging and C_{rate} is shown. Tortuosity is inversely related to porosity. Hence, the variation follows a trend but opposite to the porosity.

Fig. S.9 shows the variation of values of tortuosity for different types of charging at various C_{rates}. The lower charging rates in all the techniques showed resulted in the highest value of tortuosity. The conventional CC and CCCV have the maximum variation in the tortuosity, especially at low C_{rate}. At lower C_{rate} other parameters such as concentration of inactive materials and the SEI layer thickness is higher. The SEI layer is a type of inactive material that is formed on the surface of electrode particles. These

particles are kept together using binders and have spaces in between them, which are called pores. These pores allow the Li-ion to settle during intercalation reaction or charging. When the SEI layer thickness increases, the pores start getting clogged and restrain the movement of charges[14,86]. Hence, during charge transfer or diffusion, a larger path is required, which leads to an increase in tortuosity. Since the porosity of electrodes is related to tortuosity, the calculation also involves the value of porosity.

On the introduction of pulse charge techniques, the change in the values of tortuosity reduces as compared to CC and CCCV. The t_{on} and t_{off} have impact on the change in the tortuosity similar porosity changes shown in Fig. S.10b. The decrease in the t_{on} and t_{off} reduces the tortuosity changes due to similar reasons as described in the previous subsection explaining the less change in the porosity and SEI layer thickness. Looking at the pulse charging with discharge, the change in tortuosity over different charging rates are the least except for a low C_{rate} in CT9. CT9 has a high t_{on}, therefore at low C_{rate}, the formation of SEI to constrain the diffusivity of charge is least. On an increase of C_{rate}, the internal cell temperature increases, boosting the diffusivity of charge. Further, the increase in the amplitude of discharge pulse in pulse charging with discharge also increases the internal cell temperature. Hence, for CT13 and CT15, in which the amplitude of discharge pulse is twice the average charge current, the tortuosity changes are minimal. The pulse charge with discharge turns out to be a good alternative to fast charge batteries if the only tortuosity is considered under study.

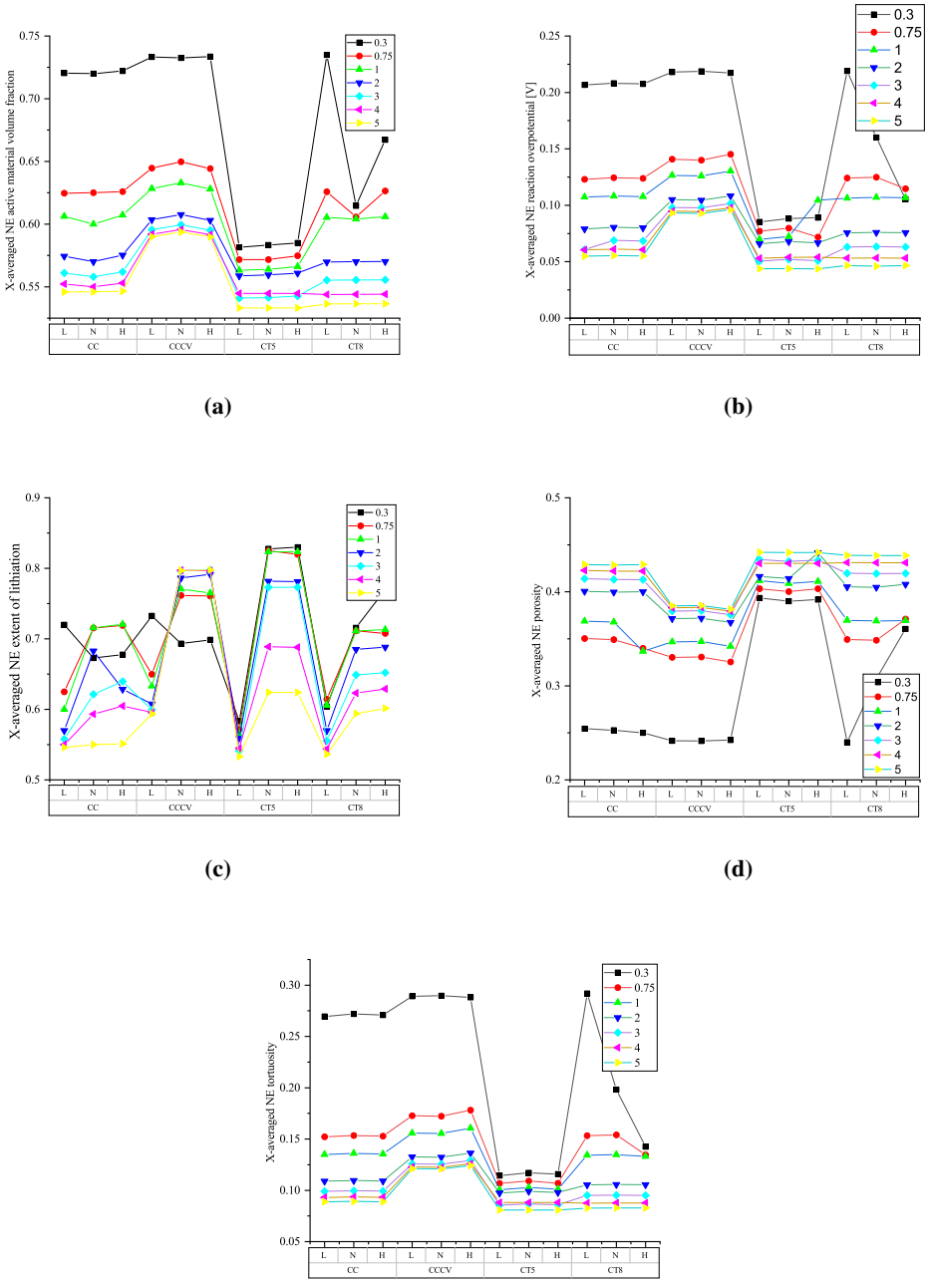

Figure S.10: Variation of different parameters of the batteries: (a) X-averaged negative electrode inactive material volume fraction; (b) X-averaged negative electrode reaction overpotential [V]; (c) X-averaged negative electrode extent of lithiation; (d) X-averaged negative electrode porosity; (e) X-averaged negative electrode tortuosity. For each parameters, shown in the figure, CT5 results a value which help to constrain the battery degradation.

Table S.3: The table shows the parameters of cell used for simulating the different types of charging at different rates. The cell parameters are taken from[18] and the additional data required for the degradation models are those predefined in PyBaMM.

Parameter	**Symbol**	**Units**	**Anode**	**Cathode**
Length of the electrode	L_i	μm	88	80
Conductivity of electrode	σ	S/m	100	100
Volume fraction of solid phase	ε_1		0.49	0.59
Volume fraction of liquid phase	ε_2		0.485	0.385
Film thickness	δ	μm	2	2
Maximum Li ion in sold phase		mol/m^3	30555	51555
State of charge	θ_0		0.03	0.95
Diffusion coefficient of solid phase	D_1	m^2/s	3.9×10^{-14}	1×10^{-14}
Rate constant of electrochemical reactions	κ	$A/m^2/(mol/m^3)^{3/2}$	4.854×10^{-6}	2.252×10^{-6}
Anodic transfer coefficient of electrochemical reactions	α_a		0.5	0.5
Anodic transfer coefficient of electrochemical reactions	α_b		0.5	0.5
Initial Li ion in sold phase		mol/m^3	1000	1000
Diffusion coefficient of liquid phase	D2	m^2/s	7.5×10^{-14}	7.5×10^{-14}
Transference number of Li ion	t^+		0.363	0.363
Faraday constant	F	$C.mol^{-1}$		
Gas constant	R	$J.mol^{-1}K^{-1}$		

Table S.4: The table shows different types of charging techniques simulated in the work. The t_{on}, t_{off} and t_{dis} are the time during a period of pulse to turn on to charge, turn off to rest and discharge, respectively. Each charging technique is simulated on a DFN model with incorporated degradation models at different charging rates. The empty spaces resembles that the specific parameter is not relevant for the charging type.

Sl.No	Charging techniques	Sub category	$t_{on}(s)$	$t_{off}(s)$	$t_{dis}(s)$
1	CC				
2	CCCV				
3	Pulse charge without discharge	Type 1	5	0.2	
4	Pulse charge without discharge	Type 2	3	0.2	
5	Pulse charge without discharge	Type 3	1	0.2	
6	Pulse charge without discharge	Type 4	5	0.1	
7	Pulse charge without discharge	Type 5	3	0.1	
8	Pulse charge without discharge	Type 6	1	0.1	
9	Pulse charge with discharge	Type 1	5	0.2	0.2
10	Pulse charge with discharge	Type 2	3	0.2	0.2
11	Pulse charge with discharge	Type 3	1	0.2	0.2
12	Pulse charge with discharge	Type 4	5	0.2	0.2
13	Pulse charge with discharge	Type 5	5	0.2	0.2
14	Pulse charge with discharge	Type 6	3	0.2	0.2
15	Pulse charge with discharge	Type 7	3	0.2	0.2